Report

Neuron

A Sensor for Low Environmental Oxygen in the Mouse Main Olfactory Epithelium

Highlights

- Sensing the level of oxygen in the external environment is essential for survival
- Low oxygen directly activates sensory neurons in the mouse main olfactory epithelium
- These responses require the guanylate cyclase Gucy1b2 and the cation channel Trpc2
- A mouse could thus rapidly assess the oxygen level in the external environment

Authors

Katherin Bleymehl, Anabel Pérez-Gómez, Masayo Omura, ..., Trese Leinders-Zufall, Frank Zufall, Peter Mombaerts

Correspondence

frank.zufall@uks.eu (F.Z.), peter.mombaerts@gen.mpg.de (P.M.)

In Brief

Sensing the level of oxygen is essential for survival, but no mammalian olfactory system has been implicated. Bleymehl et al. demonstrate that low oxygen activates mouse sensory neurons that express the soluble guanylate cyclase Gucy1b2 and the cation channel Trpc2.

Bleymehl et al., 2016, Neuron *92*, 1196–1203
December 21, 2016
http://dx.doi.org/10.1016/j.neuron.2016.11.001

CellPress

CellPress

Neuron
Report

A Sensor for Low Environmental Oxygen in the Mouse Main Olfactory Epithelium

Katherin Bleymehl,[1,5] Anabel Pérez-Gómez,[1,5] Masayo Omura,[2,5] Ana Moreno-Pérez,[1] David Macías,[3] Zhaodai Bai,[2] Randall S. Johnson,[3,4] Trese Leinders-Zufall,[1] Frank Zufall,[1,*] and Peter Mombaerts[2,6,*]

[1]Center for Integrative Physiology and Molecular Medicine, Saarland University, 66421 Homburg, Germany
[2]Max Planck Research Unit for Neurogenetics, 60438 Frankfurt, Germany
[3]Department of Physiology, Development & Neuroscience, University of Cambridge, Physiological Laboratory, Cambridge CB2 3EG, UK
[4]Department of Cell and Molecular Biology, Karolinska Institute, 171 77 Stockholm, Sweden
[5]Co-first author
[6]Lead Contact
*Correspondence: frank.zufall@uks.eu (F.Z.), peter.mombaerts@gen.mpg.de (P.M.)
http://dx.doi.org/10.1016/j.neuron.2016.11.001

SUMMARY

Sensing the level of oxygen in the external and internal environments is essential for survival. Organisms have evolved multiple mechanisms to sense oxygen. No function in oxygen sensing has been attributed to any mammalian olfactory system. Here, we demonstrate that low environmental oxygen directly activates a subpopulation of sensory neurons in the mouse main olfactory epithelium. These neurons express the soluble guanylate cyclase Gucy1b2 and the cation channel Trpc2. Low oxygen induces calcium influx in these neurons, and Gucy1b2 and Trpc2 are required for these responses. In vivo exposure of a mouse to low environmental oxygen causes Gucy1b2-dependent activation of olfactory bulb neurons in the vicinity of the glomeruli formed by axons of Gucy1b2+ sensory neurons. Low environmental oxygen also induces conditioned place aversion, for which Gucy1b2 and Trpc2 are required. We propose that this chemosensory function enables a mouse to rapidly assess the oxygen level in the external environment.

INTRODUCTION

The sense of smell relies predominantly on the repertoire of ~1,100 odorant receptor genes expressed in canonical olfactory sensory neurons (OSNs) in the main olfactory epithelium (MOE) (Buck and Axel, 1991). The mouse olfactory system comprises a variety of additional subsystems that detect a wide diversity of molecular cues in the external environment (Dey and Stowers, 2016; Munger et al., 2009). We have described a novel subpopulation of sensory neurons in the mouse MOE: type B cells (Omura and Mombaerts, 2014, 2015; Saraiva et al., 2015). Type B cells express the transient receptor potential cation channel Trpc2, thought for many years to be expressed exclusively in vomeronasal sensory neurons (VSNs), where it is a critical component of signal transduction (Leypold et al., 2002; Lucas et al., 2003; Stowers et al., 2002). Within the MOE, type B cells are unique in their expression of the soluble guanylate cyclase Gucy1b2, a molecule that is poorly characterized. We refer to Trpc2+ Gucy1b2+ neurons of the MOE as type B cells in order to distinguish them from Trpc2+ Gucy1b2− cells of the MOE (type A cells), some of which express odorant receptor genes (Omura and Mombaerts, 2014).

The functions of type B cells remain enigmatic, and no sensory stimuli have been described. Molecularly, type B cells are fundamentally different from canonical OSNs and VSNs (Omura and Mombaerts, 2014, 2015; Saraiva et al., 2015), suggesting that their ligands are also fundamentally different. First, type B cells do not appear to express odorant receptor genes, vomeronasal receptor genes, or trace amine-associated receptor genes. Second, type B cells express the cyclic nucleotide-gated channel subunit Cnga2 (characteristic for OSNs) and Trpc2 (characteristic for VSNs), but not the adenylate cyclase Adcy3 (characteristic for OSNs). Third, the differential, higher expression of 55 genes by type B cells compared to canonical OSNs defines type B cells as a cell type that is molecularly distinct from OSNs.

Here, we report the first sensory stimulus for type B cells: a reduced level of oxygen, hereafter referred to as low environmental oxygen or low oxygen. The behavioral deficits in a novel gene-targeted mouse strain carrying a knockout mutation in the *Gucy1b2* locus are consistent with a biological function of type B cells as sensors for low oxygen in the external environment.

RESULTS

Low Oxygen Directly Activates Type B Cells

Type B cells can be visualized in the MOE of mice of the gene-targeted Gucy1b2-IRES-tauGFP strain, in which *Gucy1b2* remains intact in its coding region and is coexpressed with a fusion protein of tau and GFP (Omura and Mombaerts, 2015) (Figure 1A). We hereafter abbreviate this mutant allele as Gucy1b2-GFP. To determine the chemical cues that are detected by these neurons, we dissociated the MOE of homozygous (−/−) Gucy1b2-GFP mice. This procedure yielded 0.4%–1.9% GFP-positive cells (GFP+, type B) in the dissociated cell preparations. The remaining cells are GFP negative (GFP−, non-type B). This proportion of GFP+ cells in the dissociated cell preparations is consistent with the sparse distribution

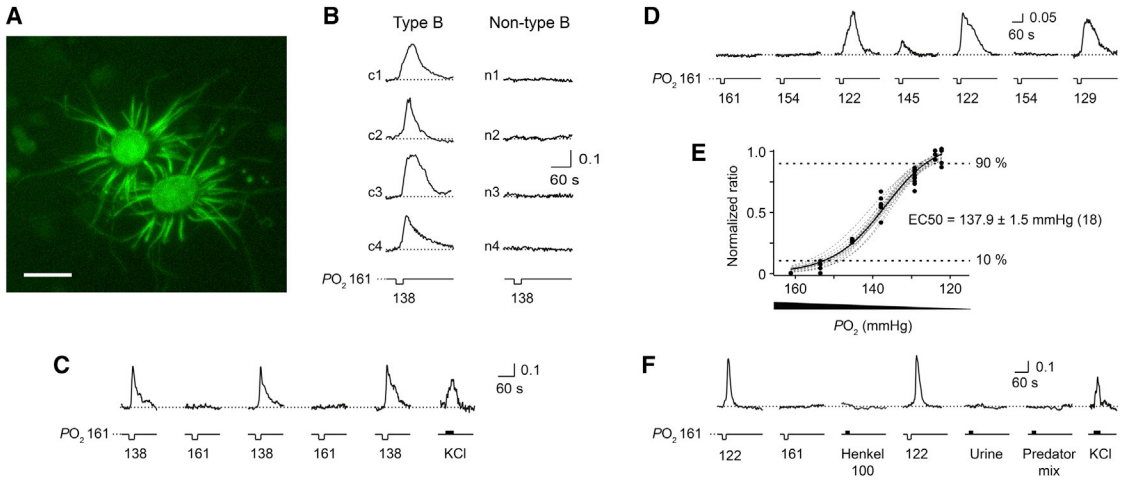

Figure 1. Type B Cells Respond to Low Oxygen

(A) Confocal image of intrinsic fluorescence of type B cells from a Gucy1b2-GFP −/− mouse (8 weeks) in an ex vivo en face whole-mount preparation. Scale bar, 5 μm.

(B) Decreasing the PO_2 from 161 to 138 mmHg in the bath solution evoked a transient rise in intracellular Ca^{2+} in type B cells within seconds. No responses occurred in non-type B cells. A Ca^{2+} response is defined as a stimulus-dependent deviation in fluorescence ratio exceeding twice the SD of the mean baseline noise.

(C) Repeatability of type B cell responses to low oxygen (138 mmHg). KCl, 30 mM.

(D) Examples of Ca^{2+} responses to various levels of low oxygen (in mmHg) in a type B cell.

(E) Stimulus-response curves obtained from single type B cells (n = 18; dashed gray lines). Each cell was stimulated with 20 s pulses of solution containing distinct oxygen levels (mmHg). Relative changes in peak fluorescence ratio induced by a given stimulus were normalized to the maximum peak fluorescence ratio of a given cell. Curves are fit using the Hill equation combined with an iterative Levenberg-Marquardt nonlinear, least-squares fitting routine, defining EC_{50}, slope (−22.9 ± 3.0), and saturation (1.0 ± 0.05). Solid black curve represents a fit of the mean stimulus-response curve using all measured data points (chi-square 0.201823; p = 0.99). Responses were recorded during a 4 min trial period with a 1 min recovery period between trials (illumination off). Each stimulus was tested one to three times per cell. Numbers are presented as mean ± SD.

(F) Responses of a type B cell to various chemostimuli. Low oxygen (122 mmHg), Henkel 100 (1:100), diluted urine (1:100), predator odor mix (TMT, [2,5-dihydro-2,4,5-trimethylthiazole], PEA [β-phenylethylamine], 2-PT [2-propylthietane], and 2,6-DMP [2,6-dimethylpyrazine], each at 100 μM), and KCl (30 mM).

of type B cells within the MOE (Omura and Mombaerts, 2014, 2015). For comparison, we also analyzed type A cells, which were identified through post hoc immunostaining with Adcy3.

We loaded the dissociated cells with the Ca^{2+} indicator fura-2/AM. We performed ratiometric Ca^{2+} imaging (Pérez-Gómez et al., 2015) in order to visualize neural activity after chemical stimulation. Cells were continuously superfused with oxygenated solution (95% O_2, 0% N_2, and 5% CO_2) yielding an O_2 tension (PO_2) of 161 mmHg (1 mmHg = 133.3 Pa), which is equivalent to a relative atmospheric O_2 level of 21.7% (Figure S1A). Under these conditions, type B cells did not show spontaneous Ca^{2+} transients but responded to elevated KCl (30 mM) with a Ca^{2+} rise. Switching for 20 s to a solution with a low oxygen level (60% O_2, 35% N_2, and 5% CO_2; yielding a PO_2 of 138 mmHg, equivalent to a relative atmospheric O_2 level of 18.6%; Figure S1A) but keeping the CO_2 level and pH constant produced a transient rise in intracellular Ca^{2+} in 69% of type B cells (142/206), whereas 0/110 non-type B cells responded to this stimulus (Figure 1B; Figure S1F). Ca^{2+} elevations in type B cells to low oxygen levels could be repeated multiple times without obvious desensitization (Figure 1C) and persisted when minutes-long stimuli were applied (Figures S1B and S1C).

Stimulus-response curves derived from 18 single type B cells (Figures 1D and 1E) allowed us to make three inferences about the oxygen-sensing mechanism. First, these curves are nearly identical, suggesting that the cells expressed an oxygen sensor with identical or very similar molecular properties. Second, the stimulus-response curves are extremely steep, with Hill coefficients of 22.95 ± 3.3; hence, their relative dynamic range is narrow, comprising a difference in O_2 levels of ~1.4 ppm (44 μM). Third, the 10%–90% operating range of these cells (153–126 mmHg; EC_{50} = 137.9 ± 1.5 mmHg) is far above the range of normal (~100 mmHg) PO_2 values in arterial blood or the working range of carotid body chemosensors, the major sensors of blood oxygen in mammals (López-Barneo et al., 2016; Prabhakar, 2016; Semenza, 2011). It is therefore unlikely that type B cells detect the level of oxygen in blood.

Type B cells also generated a Ca^{2+} rise to stimulation with 3-isobutyl-1-methylxanthine (IBMX, 100 μM), which inhibits endogenous phosphodiesterases, and to 8-bromo-cGMP (8-br-cG, 500 μM), a membrane-permeable cyclic guanosine 3′,5′ monophosphate (cGMP) analog (Figures S1D and S1F). But unlike canonical OSNs, type B cells did not respond to forskolin (50 μM), which activates adenylate cyclase (Figures S1D and S1F). Type A cells did not respond to low oxygen but responded to IBMX with a Ca^{2+} rise (Figure S1D). Several other chemostimuli failed to produce Ca^{2+} elevations in type B cells (Figure 1F; Figure S1F), including carbon disulfide (CS_2, 13 μM), a volatile semiochemical (Munger et al., 2010); mouse urine (1:100), a

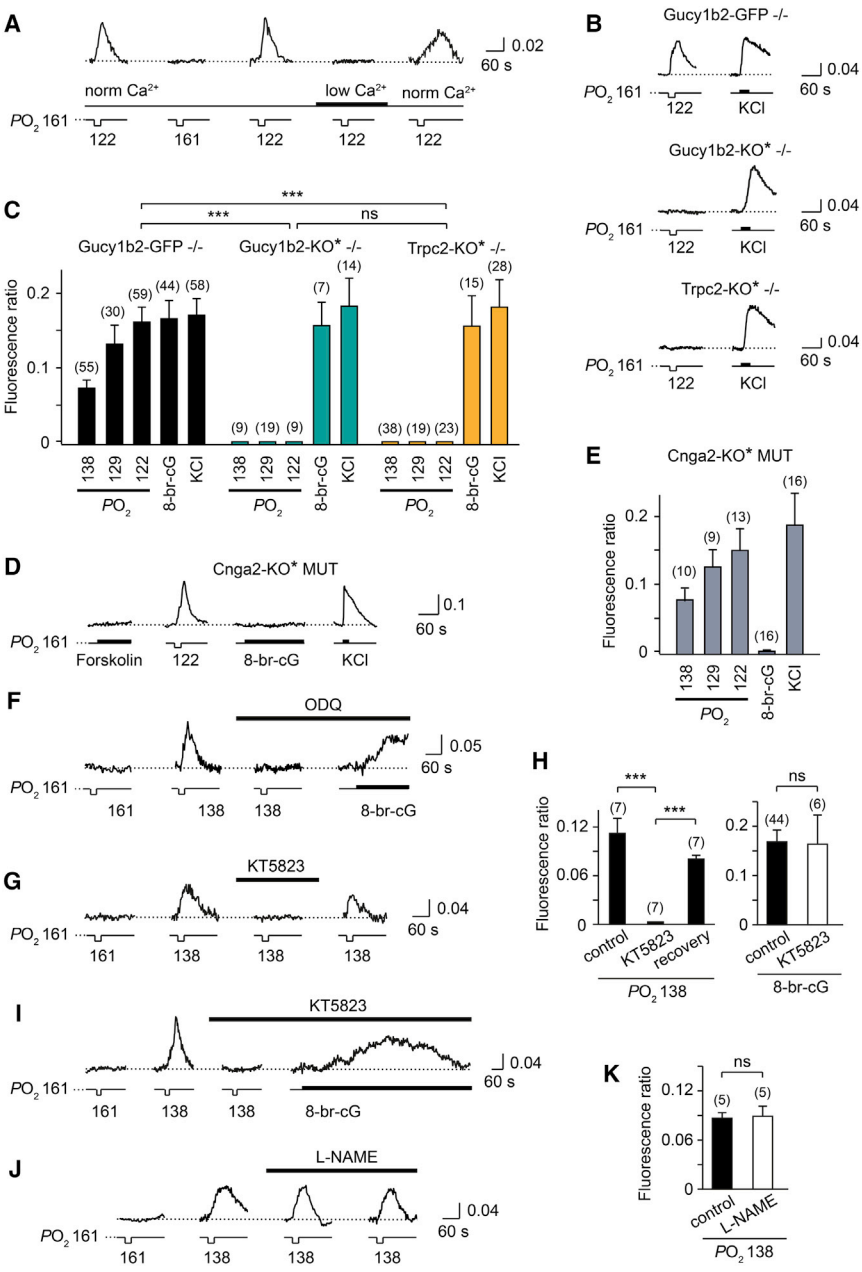

Figure 2. Low-Oxygen-Evoked Ca^{2+} Responses of Type B Cells Require Ca^{2+} Entry, Gucy1b2, and Trpc2

(A) Recording example indicating that Ca^{2+} responses to low oxygen (122 mmHg) depend on Ca^{2+} entry into type B cells. Removal of external Ca^{2+} eliminated the response in a reversible manner.

(B) Recording examples of Ca^{2+} responses in type B cells from Gucy1b2-GFP −/− mice, Gucy1b2-KO* −/− mice, and Trpc2-KO* −/− mice. Cells were stimulated with low oxygen (122 mmHg) or KCl (30 mM).

(C) Group data indicating that the Ca^{2+} responses to low oxygen require Gucy1b2 (Gucy1b2-KO* −/−, n = 4 mice) and Trpc2 (Trpc2-KO* −/−, n = 5 mice) (PO_2: 138, 129, or 122 mmHg) (ANOVA: $F(14,398) = 12.791$, $p < 0.0001$; LSD: $^*p < 0.05$, $^{**}p < 0.001$, $^{***}p < 0.0001$). Responses to 8-bromo-cGMP (8-br-cG; 500 μM) or KCl (30 mM) do not differ between the three genotypes (LSD: p = 0.66–0.71). Maximum fluorescence ratios are plotted; number of cells for each genotype and stimulus condition is indicated above each bar. No significant difference was observed between Gucy1b2-GFP −/− mice and Gucy1b2-KO* +/− mice in the responsiveness of their type B cells (n = 6; LSD: p = 0.55).

(D and E) Recording example (D) and group data (E) (n = 3 mice) indicating that type B cells in Cnga2-KO* MUT mice have normal Ca^{2+} responses to low oxygen but lack responsiveness to 8-br-cGMP (500 μM). Number of cells is indicated above each bar.

(F) Recording example indicating that Ca^{2+} responses to low oxygen in a type B cell (Gucy1b2-GFP −/− mouse) are eliminated after a 10 min treatment with ODQ (10 μM) (paired t test: $t = 3.835$, $^*p < 0.05$), whereas the response to 8-br-cGMP (500 μM) is not.

(G–I) Recording examples (G and I) and group data (H) showing the effects of the PKG inhibitor KT5823 (10 μM) on type B cell Ca^{2+} responses to low oxygen (138 mmHg) or 8-br-cGMP (50 μM). Responses to low oxygen are blocked by KT5823 in a reversible manner (ANOVA: $F(2,20) = 26.856$, $p < 0.0001$; LSD: $^{***}p < 0.0001$), whereas responses to 8-br-cGMP remain unaffected (p = 0.17). Number of independent recordings is indicated above each bar.

(J and K) Lack of effect of the NOS inhibitor L-NAME (100 μM) on type B cell Ca^{2+} responses to low oxygen (138 mmHg) (paired t test: $t = 2.359$, p = 0.078).

Results in histograms are presented as mean ± SEM.

rich source of natural pheromones; a mixture containing 100 volatile odorants (Henkel 100, 1:100); and a mixture containing four volatile predator odors (Pérez-Gómez et al., 2015). Moreover, type B cells did not respond to shifting the proton (H^+) concentration in the solution to values of pH 6.5 or 7.5 (Figures S1E and S1F). Taken together, low oxygen generates rapid, graded, and seemingly non-adapting responses in type B cells.

Gucy1b2 and Trpc2 Are Required for Type B Cell Responses to Low Oxygen

Next, we investigated the mechanistic basis of low-oxygen-evoked Ca^{2+} rises in type B cells.

Removal of extracellular Ca^{2+} abolished the responses in a reversible manner, indicating that responses were triggered primarily by Ca^{2+} entry into the cells (Figure 2A; Figure S1H). To determine whether Gucy1b2 is essential for the evoked

responses in type B cells, we generated a novel mouse strain with a gene-targeted knockout (KO) in the *Gucy1b2* gene, Gucy1b2-D-IRES-tauGFP (hereafter abbreviated as Gucy1b2-KO). Because the *GFP* sequence is spliced out of the mutant transcripts, the cells expressing the mutant allele do not express GFP (Figure S2). Therefore we crossed the Gucy1b2-KO mutation with the gene-targeted Trpc2-IRES-taumCherry mutation (Omura and Mombaerts, 2014), in which *Trpc2* is intact in its coding sequence and coexpressed with a fusion of tau and mCherry. Mice of this cross are referred to as Gucy1b2-KO*, with the asterisk referring to the intrinsic fluorescence of mCherry. Gucy1b2-KO* mice can be heterozygous (+/−) or homozygous (−/−) for the Gucy1b2-KO mutation but are always homozygous for Trpc2-IRES-taumCherry and are referred to as, respectively, Gucy1b2-KO* +/− or Gucy1b2-KO* −/−. In mice of this cross, we performed post hoc immunostaining (Chamero et al., 2011) for Adcy3 to distinguish type B cells (which are Adcy3− and mCherry+) from type A cells (which are Adcy3+ and mCherry+); canonical OSNs are Adcy3+ and mCherry− (Figure S1G). We found that low-oxygen-evoked Ca^{2+} rises were abolished in type B cells from Gucy1b2-KO* −/− mice, whereas responses to 8-bromo-cGMP or KCl remained normal (Figures 2B and 2C).

Next, we performed similar experiments in mice that are homozygous for Gucy1b2-GFP and homozygous for a knockout mutation in the *Trpc2* gene (Trpc2-KO) (Omura and Mombaerts, 2014). These doubly homozygous mice are referred to as Trpc2-KO* −/− mice, with the asterisk referring to the intrinsic fluorescence of GFP. Here, too, we found that low-oxygen-evoked Ca^{2+} rises were abolished in type B cells from Trpc2-KO* −/− mice, whereas responses to 8-bromo-cGMP or KCl remained normal (Figures 2B and 2C). These results identify both Gucy1b2 and Trpc2 as essential molecular components of the signal transduction machinery that underlies the sensing of low oxygen by type B cells.

To determine whether Cnga2 is required for low-oxygen-evoked Ca^{2+} elevations in type B cells, we performed experiments in mice that are homozygous for Trpc2-IRES-taumCherry and hemizygous (males) or homozygous (females) for a knockout mutation in the *Cnga2* gene, which is located on the X chromosome (Zheng et al., 2000). Mice of this cross are referred to as Cnga2-KO* MUT, with the asterisk referring to the intrinsic fluorescence of mCherry and MUT referring collectively to mice that are hemizygous or homozygous for the *Cnga2* knockout mutation. Low-oxygen-evoked Ca^{2+} rises and responses to KCl remained normal in type B cells of Cnga2-KO* MUT mice, whereas responses to 8-bromo-cGMP were absent (Figures 2D and 2E). Thus, Cnga2 is not required for the sensing of low oxygen by type B cells but is required for producing a Ca^{2+} elevation to 8-bromo-cGMP application. Therefore, Trpc2, but not Cnga2, is the critical ion channel for the generation of low-oxygen-evoked Ca^{2+} responses in type B cells.

Atypical soluble guanylate cyclases of invertebrates contain heme-nitric oxide and oxygen-binding domains that can form a stable complex with oxygen (Derbyshire and Marletta, 2012; Gray et al., 2004; Morton, 2004). We applied ODQ (10 μM), a chemical that targets such domains and inhibits soluble guanylate cyclases by oxidation of the ferrous iron in the heme cofactor (Derbyshire and Marletta, 2012). We observed that low-oxygen-evoked responses of type B cells were eliminated following ODQ treatment (Figure 2F; Figure S1J). Thus, heme-nitric oxide and oxygen-binding domains are required for the sensing of low oxygen by type B cells, consistent with the requirement for Gucy1b2.

Rat Gucy1b2, which exhibits a high amino acid sequence identity to mouse Gucy1b2, can be enzymatically active and produce cGMP in the absence of another subunit (Koglin et al., 2001). One potential route of how cGMP formation can evoke neuronal excitation is through phosphorylation via a cGMP-activated protein kinase (PKG). Low-oxygen-evoked responses of type B cells were eliminated in a reversible manner following treatment with the PKG inhibitor KT5823 (10 μM) (Figures 2G and 2H). This result indicates that a PKG is required for the sensing of low oxygen in type B cells and also argues that a rise in intracellular cGMP concentration underlies this response. Interestingly, the Ca^{2+} elevation to 8-bromo-cGMP remained normal after KT5823 treatment (Figures 2I and 2H), consistent with a model in which Trpc2 and Cnga2 are part of two independent signaling pathways in type B cells (see Discussion).

We assessed a role of endogenously produced nitric oxide (NO) in the response to low oxygen by inhibiting NO synthases (NOS) with the cell-permeable NOS inhibitor L-NAME (100 μM). This treatment had no effect on low-oxygen-evoked responses in type B cells (Figures 2J and 2K). Additionally, single-cell RNA sequencing (RNA-seq) analyses of type B cells revealed that these neurons do not express *Nos1*, *Nos2*, and *Nos3* (Saraiva et al., 2015). Together, these results rule out an involvement of endogenous NO produced through NOS activity in the sensing of low oxygen by type B cells.

Low Oxygen Activates Olfactory Bulb Neurons in the Vicinity of Type B Cell Glomeruli in Freely Breathing Mice

Based on the results of the single-cell experiments, we surmised that type B cells serve as sensitive detectors of reduced oxygen levels in the ambient air—environmental hypoxia. The axons of type B cells terminate in approximately three glomeruli on the posteroventral surface of the main olfactory bulb near the necklace glomeruli (Omura and Mombaerts, 2014, 2015), where they synapse onto olfactory bulb neurons. Type B cell glomeruli can be visualized in mice that are heterozygous or homozygous for the Gucy1b2-GFP mutation (Omura and Mombaerts, 2015). We assessed activation of postsynaptic olfactory bulb neurons in the vicinity of type B cell glomeruli following exposure of mice to low environmental oxygen by using immunohistochemistry for the immediate early gene product c-Fos (Pérez-Gómez et al., 2015) (Figure 3). Singly housed mice of three genotypes (Gucy1b2-GFP −/− mice used as reference mice, Gucy1b2-KO* +/− mice, and Gucy1b2-KO* −/− mice) were habituated to 20% O_2 in a testing arena for 30 min each day for 3 consecutive days. On day 4, mice were exposed to 20% O_2 for 30 min and subsequently to either 16% or 20% O_2 for an additional 10 min. Gucy1b2-GFP −/− mice responded to low oxygen exposure with a robust increase in the number of c-Fos immunoreactive cells that reside in the vicinity of type B cell glomeruli (Figures 3A, 3B, and 3G). Similar results were obtained

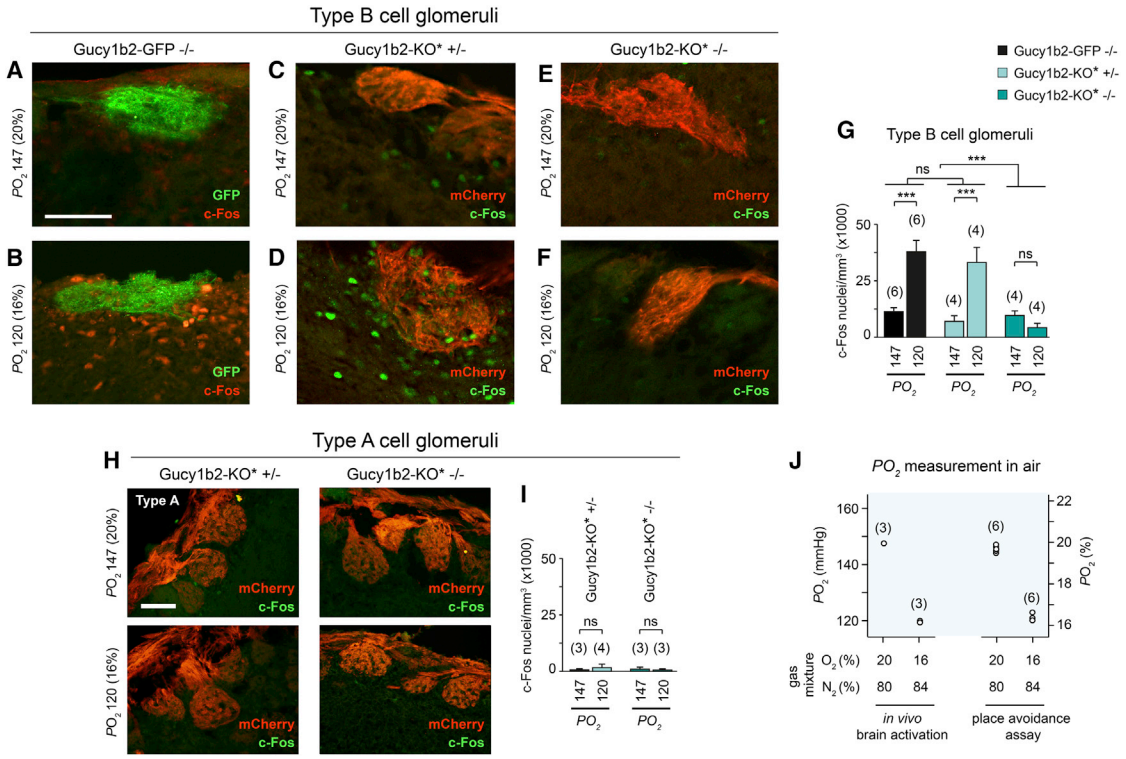

Figure 3. Low Environmental Oxygen Causes Gucy1b2-Dependent Activation of Olfactory Bulb Neurons in the Vicinity of Type B Cell Glomeruli in Freely Breathing Mice

(A–F) c-Fos immunoreactivity in the olfactory bulbs of Gucy1b2-GFP −/− mice (A and B), of Gucy1b2-KO* +/− mice (C and D), and of Gucy1b2-KO* −/− mice (E and F). Mice were exposed to normal (147 mmHg, 20%) (A, C, and E) or low (120 mmHg, 16%) (B, D, and F) oxygen. Sagittal sections were derived from olfactory bulbs. The intrinsic fluorescence of GFP or the immunoreactivity for mCherry identifies presynaptic axons and outlines the dense glomerular neuropil. The c-Fos immunoreactivity denotes the activity of postsynaptic olfactory bulb neurons. Scale bar, 50 μm.

(G) Quantification of c-Fos+ nuclei reveals that exposure to low environmental oxygen caused a significant increase in neuronal activity in the vicinity of type B cell glomeruli of Gucy1b2-GFP −/− mice (used as reference mice) and Gucy1b2-KO* +/− mice. Responses in these two genotypes were indistinguishable from each other (LSD: $p = 0.95$). By contrast, this response was absent in Gucy1b2-KO* −/− mice (LSD: $p = 0.14$). ANOVA genotype: $F(2,229) = 28.767$, $p < 0.0001$; ANOVA treatment: $F(1,229) = 105.600$, $p < 0.0001$; LSD: ***$p < 0.0001$. The number of sections analyzed ranged from 23 to 57 per genotype and treatment. Number of mice is indicated above each bar.

(H) c-Fos immunoreactivity in the vicinity of type A cell glomeruli in the olfactory bulbs of Gucy1b2-KO* +/− mice (left panels) and Gucy1b2-KO* −/− mice (right panels). Mice were exposed to normal (147 mmHg, 20%) or low (120 mmHg, 16%) oxygen. Scale bar, 50 μm. No c-Fos immunoreactivity was detetectable under these conditions.

(I) Quantification of c-Fos+ nuclei reveals that exposure to low oxygen caused no significant increase in neuronal activity in the vicinity of type A cell glomeruli of Gucy1b2-KO* +/− or Gucy1b2-KO* −/− mice (ANOVA: $F(1,251) = 0.134$, $p = 0.72$). Basal c-Fos immunoreactivity was very low, and the two genotypes were indistinguishable from each other (ANOVA: $F(1,251) = 2.712$, $p = 0.10$). The number of sections analyzed ranged from 18 to 124 per genotype and treatment. Number of mice is indicated above each bar.

(J) Plot of the oxygen levels measured in the ambient air of the behavioral chambers as used during in vivo experiments of activation of olfactory bulb neurons and conditioned place aversion. Concentrations were measured in percentage and converted into PO_2 (mmHg). Number of independent measurements is indicated. PCO_2 was <0.1% (0.76 mmHg).

Results in histograms are presented as mean ± SEM.

in Gucy1b2-KO* +/− mice (Figures 3C, 3D, and 3G), but this response was abolished in Gucy1b2-KO* −/− mice (Figures 3E–3G).

We also assessed the specificity of type B cell glomeruli versus type A cell glomeruli in their responsivity to low oxygen exposure. Type A cell glomeruli reside at rostral positions on the ventral surface of the main olfactory bulb and can be visualized in heterozygous or homozygous Trp2-IRES-taumCherry mice (Omura and Mombaerts, 2014, 2015). In contrast to type B cell glomeruli, we found no evidence that postsynaptic olfactory bulb neurons in the vicinity of type A cell glomeruli were activated following in vivo exposure to low oxygen either in Gucy1b2-KO* +/− or in Gucy1b2-KO* −/− mice (Figures 3H and 3I). These in vivo results are consistent with our Ca^{2+} imaging experiments on single type A cells (Figure S1D) and confirm and extend our observations that low-oxygen-evoked responses occur in type B cells, but not in type A cells.

These results demonstrate the physiological relevance of low oxygen detection by type B cells in awake, behaving mice and link the sensing of low environmental oxygen to type B cells in a biologically relevant context.

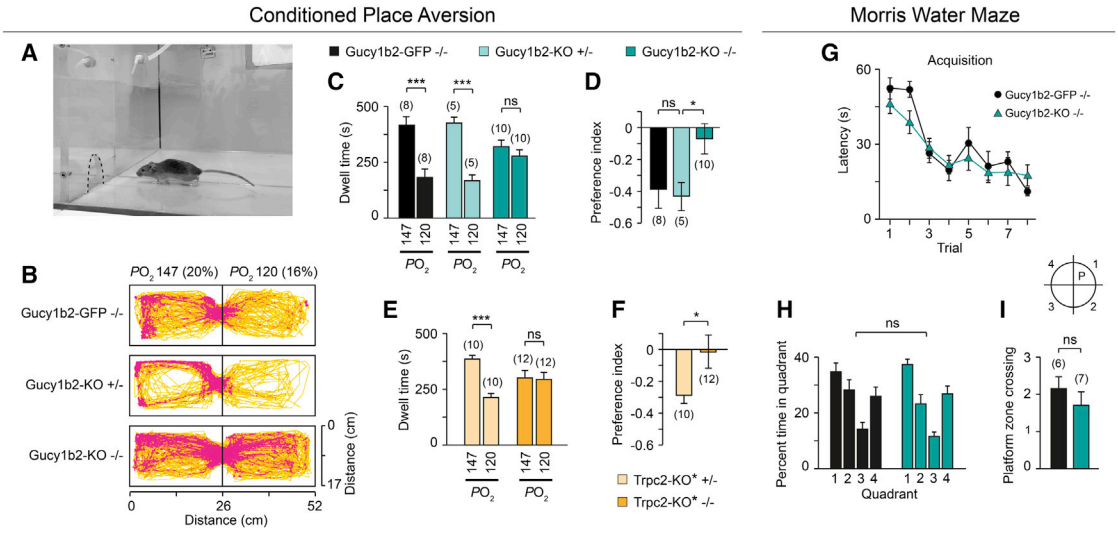

Figure 4. Gucy1b2 and Trpc2 Are Required for Conditioned Place Aversion of a Low-Oxygen Environment

(A) Behavioral arena. The opening between the two chambers is indicated with a stipple line. Experiments were performed under infrared illumination.

(B) Heatmap graphs obtained from trajectory plots of all tested mice in the conditioned place aversion assay demonstrating their preference of the 20%-paired chamber versus the 16%-paired chamber.

(C and D) Average dwell times and preference index of Gucy1b2-GFP −/− mice (used as reference mice), Gucy1b2-KO +/− mice and Gucy1b2-KO −/− mice for the 20%- versus 16%-paired chamber. ANOVA: $F(5,22) = 3.728$, $p < 0.042$; LSD: $^{**}p < 0.001$; n.s., $p = 0.79$ (C); ANOVA: $F(5,45) = 10.256$, $p < 0{,}002$; LSD: $^{**}p < 0.001$; n.s., $p = 0.28$) (D).

(E and F) Average dwell times and preference index of Trpc2-KO* +/− mice and Trpc2-KO* −/− mice for the 20%- versus the 16%-paired chamber. ANOVA: $F(3,40) = 6.7629$, $p < 0.001$; LSD: $^{***}p < 0.001$; n.s., $p = 0.81$ (E); paired t test: $t(20) = 2.2353$, $^{*}p < 0.05$ (F). The number of mice is indicated at each bar.

(G) Plot of latency-to-find platform versus trial number in a Morris water maze assay for Gucy1b2-GFP −/− mice (n = 6) and Gucy1b2-KO −/− mice (n = 7). ANOVA genotype: $F(1,103) = 1.22$, $p = 0.27$.

(H and I) Analysis of reference memory in a Morris water maze assay using single probe trials in the absence of the platform (P) for Gucy1b2-GFP −/− mice (n = 6) and Gucy1b2-KO −/− mice (n = 7). Percentage of time spent in each quadrant (H; ANOVA genotype: $F(1,51) = 0.043$, $p = 0.84$) and number of platform zone crossings in quadrant 1 (I; t test: $t(11) = 0.364$, $p = 0.72$) were analyzed.

Results are presented as mean ± SEM.

Gucy1b2 and Trpc2 Are Required for Conditioned Place Aversion of a Low-Oxygen Environment

Given the importance of the olfactory system in mediating a variety of aversive behaviors (Li and Liberles, 2015; Pérez-Gómez et al., 2015), we reasoned that exposure to low environmental oxygen may evoke an aversive response. We developed a conditioned place aversion assay in order to determine whether low oxygen has negative (aversive) motivational effects. A conditioned place aversion assay is a Pavlovian conditioning task established to capture the negative reinforcement that is associated with a given stimulus or environmental cue (Cunningham et al., 2006). We determined that this test can reveal an aversive quality of low (16%) versus normal (20%) environmental oxygen levels as follows. Mice were tested in a two-chamber apparatus (Figures 4A and 4B) in which they were trained daily for 3 days to associate 16% O_2 with one chamber. On the testing day, their preference of the 16%-paired chamber (but now at 20% O_2) was quantified. Gucy1b2-GFP −/− mice (used as reference mice) and Gucy1b2-KO +/− mice spent significantly more time in the 20%-paired chamber than in the 16%-paired chamber; this difference in dwell time yields a negative preference index, which represents an aversion of the low-oxygen environment (Figures 4B–4D). By contrast, Gucy1b2-KO −/− mice failed to show a preference between the two chambers, indicating that Gucy1b2 is required for conditioned place aversion of low oxygen (Figures 4B–4D). Trpc2-KO* −/− mice also failed to display a preference for the 16%- versus the 20% O_2-paired chamber in the assay, whereas Trpc2-KO* +/− mice showed a significant preference for the 20% O_2-paired chamber (Figures 4E and 4F). The requirement for Gucy1b2 and Trpc2 in this conditioned place aversion is consistent with a biological role of type B cells in sensing a low oxygen level in the ambient air.

To exclude that this behavioral phenotype may be caused by learning and memory deficits, we performed a Morris water maze assay (Vorhees and Williams, 2006) using Gucy1b2-GFP −/− mice and Gucy1b2-KO −/− mice. We analyzed the acquisition performance measured as latency to reach the platform (Figure 4G). We observed no significant difference in the performance between the two genotypes in this test. We also assessed the reference memory using single probe trials in the absence of the platform. We analyzed the time spent in each quadrant (Figure 4H) and the number of times crossing the area where the platform used to be located (Figure 4I). Again, there was no significant difference between the two genotypes. Therefore, Gucy1b2-KO −/− mice perform normally in a place learning assay, form and keep spatial memories, and exhibit proper spatial navigation.

If Gucy1b2 expression were to also occur in neurons of the central nervous system, it may influence the interpretation of the behavioral experiments with the Gucy1b2-KO −/− mice. We analyzed selected brain regions for intrinsic GFP fluorescence using coronal sections from Gucy1b2-GFP −/− mice. This anatomical analysis included the piriform cortex, subdivisons of the amygdala, various hypothalamic nuclei, the hippocampus, the bed nucleus of the stria terminalis, the periaqueductal gray, and the nucleus accumbens (Figure S3). The absence of GFP expression in these brain regions strengthens the functional link between the activation of type B cells by low environmental oxygen and conditioned place aversion.

Last, we performed whole-body plethysmography (Macías et al., 2014) to analyze a variety of standard respiratory parameters using unrestrained mice of three genotypes: Gucy1b2-KO −/− mice, Trpc2-KO −/− mice, and wild-type 129S6/SvEvTac mice used as reference mice (Figure S4). We found that Gucy1b2 and Trpc2 are not required for the hyperventilation response to low environmental oxygen (10% O_2), indicating that Gucy1b2 and Trpc2 are not required for carotid body responses.

DISCUSSION

Here, we have revealed a novel and unexpected role of the mouse olfactory system in sensing a low oxygen level in the ambient air. We have identified a neuronal subpopulation of the MOE with previously unknown function, type B cells, as sensors of low oxygen in the external environment. The physiological responses of these cells rely on signal transduction mechanisms that require Gucy1b2 and Trpc2 and that differ fundamentally from all previously identified oxygen sensors in mammals, including the glomus cells of the carotid body. Similar to what is the case for some invertebrate soluble guanylate cyclases, a heme domain of Gucy1b2 may bind molecular oxygen, but heterologous expression or functional gene transfer, combined with mutagenesis, will be required to test this hypothesis.

Our results suggest a model in which Trpc2 and Cnga2 are part of two independent signaling pathways. One pathway is activated by low oxygen and requires Gucy1b2, PKG, and Trpc2, and another pathway requires Cnga2, with unknown upstream signaling elements and stimulus detection properties. As both pathways probably depend on cGMP signaling, they may operate in spatially segregated compartments of type B cells. The finding that 8-bromo-cGMP application did not mimic activation of the Gucy1b2-dependent pathway may be explained by the fact that not all PKG isozymes are activated effectively by 8-bromo-cGMP (Francis et al., 2010). An obvious advantage of such a parallel signaling arrangement is that it would enable a multitasking capacity of the molecular networks formed by Gucy1b2, Trpc2, and Cnga2. We speculate that other chemical cues may be sensed by these neurons as well.

In freely breathing, awake, behaving mice, we find that a low oxygen level in the ambient air mediates an aversive behavioral response—conditioned place aversion—for which Gucy1b2 and Trpc2 are required. Conditional knockouts of *Gucy1b2* or *Trpc2* exclusively in type B cells will be needed to demonstrate that this behavior is mediated exclusively by these cells. Such experiments await the identification of a type B cell-specific promoter or locus to generate a Cre driver mouse strain with the appropriate specificity. For now, our interpretation of the lack of discrimination between 16% and 20% in Gucy1b2 knockout mice and in Trpc2 knockout mice is that these behavioral deficits are fully consistent with the biological role of type B cells that we propose in detecting a reduced oxygen level in the ambient air. This aversive behavior would enable a mouse to assess external environments with differing oxygen levels and to stay within a preferred environment. As virtually all rodents, including mice, display burrowing behavior and use burrows as a defense against predators and as a safe place to rear young (Deacon, 2006), peripheral sensing of low oxygen by type B cells may contribute to identifying and remembering appropriate locations for burrowing and nest building.

In invertebrates, changes in O_2 levels in the external environment are detected by atypical soluble guanylate cyclases (Scott, 2011). In the nematode *Caenorhabditis elegans*, distinct guanylate cyclase genes (*gcy-35/36* and *gcy-31/33*) are expressed in two pairs of sensory neurons that function in opposing directions to select an environment with a preferred O_2 level; the cGMP-generating enzymes are activated by O_2 increases or decreases, respectively (Cheung et al., 2005; Gray et al., 2004; Zimmer et al., 2009). In *Drosophila melanogaster*, O_2-sensitive guanylate cyclaces mediate feeding and escape behaviors to hypoxic or hyperoxic environments (Vermehren-Schmaedick et al., 2010). Thus, nematodes and fruitflies sense O_2 levels below and above a particular setpoint or range and have developed sensors for hypoxia and hyperoxia. In terrestrial mammals, such as mice, the preferred O_2 level is presumably the atmospheric level of 21%, so it makes evolutionarily sense to develop sensors only for hypoxic conditions. We note that *GUCY1B2* and *TRPC2* are pseudogenes in human.

CONCLUSION

Type B cells may enable a mouse to rapidly assess the oxygen level in the external environment well before its arterial blood has become hypoxic and its survival is compromised. This peripheral oxygen-sensing system may influence certain social behaviors, such as nest building and other parenting behaviors, because newborns are particularly liable to suffer from hypoxia. Our study also establishes the first physiological and biological function for Trpc2 expression outside VSNs.

EXPERIMENTAL PROCEDURES

All mouse experiments and animal care were performed in accordance with institutional and national guidelines and regulations.

SUPPLEMENTAL INFORMATION

Supplemental Information includes Supplemental Experimental Procedures and four figures and can be found with this article online at http://dx.doi.org/10.1016/j.neuron.2016.11.001.

AUTHOR CONTRIBUTIONS

M.O., T.L.-Z., F.Z., and P.M. conceived the project; K.B. performed calcium imaging and post hoc immunostaining; A.P.-G. and A.M.-P. carried out c-Fos analysis; A.P.-G. performed behavioral analysis; A.P.-G. and T.L.-Z.

carried out analysis of brain sections; M.O. and Z.B. carried out the generation of Gucy1b2 knockout mice and anatomical analysis; M.O. performed en face imaging; D.M. performed whole-body plethysmography; R.S.J., T.L.-Z., F.Z., and P.M. provided supervision, expertise, and data analysis. F.Z. and P.M. wrote the manuscript.

ACKNOWLEDGMENTS

We thank Pablo Chamero for assistance during an early phase of this project and Eugenia Eckstein and Andreas Schmid for help with confocal imaging. This work was supported by Deutsche Forschungsgemeinschaft Grants SFB 894 (to T.L.-Z. and F.Z.), SFB-Transregio 152 (to T.L.-Z. and F.Z.), International Graduate School GK1326 (to F.Z.), and Schwerpunktprogramm 1392 (to T.L.-Z., F.Z., and P.M.); the Volkswagen Foundation (to T.L.-Z.; VolkswagenStiftung I/82781); the Wellcome Trust (to R.S.J.; WT092738MA); and the European Research Council Advanced Grant ORGENECHOICE (to P.M.) and the Max Planck Society (to P.M.). T.L.-Z. is a Lichtenberg Professor of the Volkswagen Foundation.

Received: July 26, 2016
Revised: September 21, 2016
Accepted: October 20, 2016
Published: December 1, 2016

REFERENCES

Buck, L., and Axel, R. (1991). A novel multigene family may encode odorant receptors: a molecular basis for odor recognition. Cell *65*, 175–187.

Chamero, P., Katsoulidou, V., Hendrix, P., Bufe, B., Roberts, R., Matsunami, H., Abramowitz, J., Birnbaumer, L., Zufall, F., and Leinders-Zufall, T. (2011). G protein G(α)o is essential for vomeronasal function and aggressive behavior in mice. Proc. Natl. Acad. Sci. USA *108*, 12898–12903.

Cheung, B.H., Cohen, M., Rogers, C., Albayram, O., and de Bono, M. (2005). Experience-dependent modulation of C. elegans behavior by ambient oxygen. Curr. Biol. *15*, 905–917.

Cunningham, C.L., Gremel, C.M., and Groblewski, P.A. (2006). Drug-induced conditioned place preference and aversion in mice. Nat. Protoc. *1*, 1662–1670.

Deacon, R.M. (2006). Burrowing in rodents: a sensitive method for detecting behavioral dysfunction. Nat. Protoc. *1*, 118–121.

Derbyshire, E.R., and Marletta, M.A. (2012). Structure and regulation of soluble guanylate cyclase. Annu. Rev. Biochem. *81*, 533–559.

Dey, S., and Stowers, L. (2016). Think you know how smell works? Sniff again. Cell *165*, 1566–1567.

Francis, S.H., Busch, J.L., Corbin, J.D., and Sibley, D. (2010). cGMP-dependent protein kinases and cGMP phosphodiesterases in nitric oxide and cGMP action. Pharmacol. Rev. *62*, 525–563.

Gray, J.M., Karow, D.S., Lu, H., Chang, A.J., Chang, J.S., Ellis, R.E., Marletta, M.A., and Bargmann, C.I. (2004). Oxygen sensation and social feeding mediated by a *C. elegans* guanylate cyclase homologue. Nature *430*, 317–322.

Koglin, M., Vehse, K., Budaeus, L., Scholz, H., and Behrends, S. (2001). Nitric oxide activates the β 2 subunit of soluble guanylyl cyclase in the absence of a second subunit. J. Biol. Chem. *276*, 30737–30743.

Leypold, B.G., Yu, C.R., Leinders-Zufall, T., Kim, M.M., Zufall, F., and Axel, R. (2002). Altered sexual and social behaviors in trp2 mutant mice. Proc. Natl. Acad. Sci. USA *99*, 6376–6381.

Li, Q., and Liberles, S.D. (2015). Aversion and attraction through olfaction. Curr. Biol. *25*, R120–R129.

López-Barneo, J., González-Rodríguez, P., Gao, L., Fernández-Agüera, M.C., Pardal, R., and Ortega-Sáenz, P. (2016). Oxygen sensing by the carotid body: mechanisms and role in adaptation to hypoxia. Am. J. Physiol. Cell Physiol. *310*, C629–C642.

Lucas, P., Ukhanov, K., Leinders-Zufall, T., and Zufall, F. (2003). A diacylglycerol-gated cation channel in vomeronasal neuron dendrites is impaired in TRPC2 mutant mice: mechanism of pheromone transduction. Neuron *40*, 551–561.

Macías, D., Fernández-Agüera, M.C., Bonilla-Henao, V., and López-Barneo, J. (2014). Deletion of the von Hippel-Lindau gene causes sympathoadrenal cell death and impairs chemoreceptor-mediated adaptation to hypoxia. EMBO Mol. Med. *6*, 1577–1592.

Morton, D.B. (2004). Atypical soluble guanylyl cyclases in *Drosophila* can function as molecular oxygen sensors. J. Biol. Chem. *279*, 50651–50653.

Munger, S.D., Leinders-Zufall, T., and Zufall, F. (2009). Subsystem organization of the mammalian sense of smell. Annu. Rev. Physiol. *71*, 115–140.

Munger, S.D., Leinders-Zufall, T., McDougall, L.M., Cockerham, R.E., Schmid, A., Wandernoth, P., Wennemuth, G., Biel, M., Zufall, F., and Kelliher, K.R. (2010). An olfactory subsystem that detects carbon disulfide and mediates food-related social learning. Curr. Biol. *20*, 1438–1444.

Omura, M., and Mombaerts, P. (2014). Trpc2-expressing sensory neurons in the main olfactory epithelium of the mouse. Cell Rep. *8*, 583–595.

Omura, M., and Mombaerts, P. (2015). Trpc2-expressing sensory neurons in the mouse main olfactory epithelium of type B express the soluble guanylate cyclase Gucy1b2. Mol. Cell. Neurosci. *65*, 114–124.

Pérez-Gómez, A., Bleymehl, K., Stein, B., Pyrski, M., Birnbaumer, L., Munger, S.D., Leinders-Zufall, T., Zufall, F., and Chamero, P. (2015). Innate predator odor aversion driven by parallel olfactory subsystems that converge in the ventromedial hypothalamus. Curr. Biol. *25*, 1340–1346.

Prabhakar, N.R. (2016). O_2 and CO_2 detection by the carotid and aortic bodies. In Chemosensory Transduction: The Detection of Odors, Tastes, and Other Chemostimuli, F. Zufall and S.D. Munger, eds. (Academic Press), pp. 321–338.

Saraiva, L.R., Ibarra-Soria, X., Khan, M., Omura, M., Scialdone, A., Mombaerts, P., Marioni, J.C., and Logan, D.W. (2015). Hierarchical deconstruction of mouse olfactory sensory neurons: from whole mucosa to single-cell RNA-seq. Sci. Rep. *5*, 18178.

Scott, K. (2011). Out of thin air: sensory detection of oxygen and carbon dioxide. Neuron *69*, 194–202.

Semenza, G.L. (2011). Oxygen sensing, homeostasis, and disease. N. Engl. J. Med. *365*, 537–547.

Stowers, L., Holy, T.E., Meister, M., Dulac, C., and Koentges, G. (2002). Loss of sex discrimination and male-male aggression in mice deficient for TRP2. Science *295*, 1493–1500.

Vermehren-Schmaedick, A., Ainsley, J.A., Johnson, W.A., Davies, S.A., and Morton, D.B. (2010). Behavioral responses to hypoxia in Drosophila larvae are mediated by atypical soluble guanylyl cyclases. Genetics *186*, 183–196.

Vorhees, C.V., and Williams, M.T. (2006). Morris water maze: procedures for assessing spatial and related forms of learning and memory. Nat. Protoc. *1*, 848–858.

Zheng, C., Feinstein, P., Bozza, T., Rodriguez, I., and Mombaerts, P. (2000). Peripheral olfactory projections are differentially affected in mice deficient in a cyclic nucleotide-gated channel subunit. Neuron *26*, 81–91.

Zimmer, M., Gray, J.M., Pokala, N., Chang, A.J., Karow, D.S., Marletta, M.A., Hudson, M.L., Morton, D.B., Chronis, N., and Bargmann, C.I. (2009). Neurons detect increases and decreases in oxygen levels using distinct guanylate cyclases. Neuron *61*, 865–879.

Neuron, Volume *92*

Supplemental Information

A Sensor for Low Environmental Oxygen in the Mouse Main Olfactory Epithelium

Katherin Bleymehl, Anabel Pérez-Gómez, Masayo Omura, Ana Moreno-Pérez, David Macías, Zhaodai Bai, Randall S. Johnson, Trese Leinders-Zufall, Frank Zufall, and Peter Mombaerts

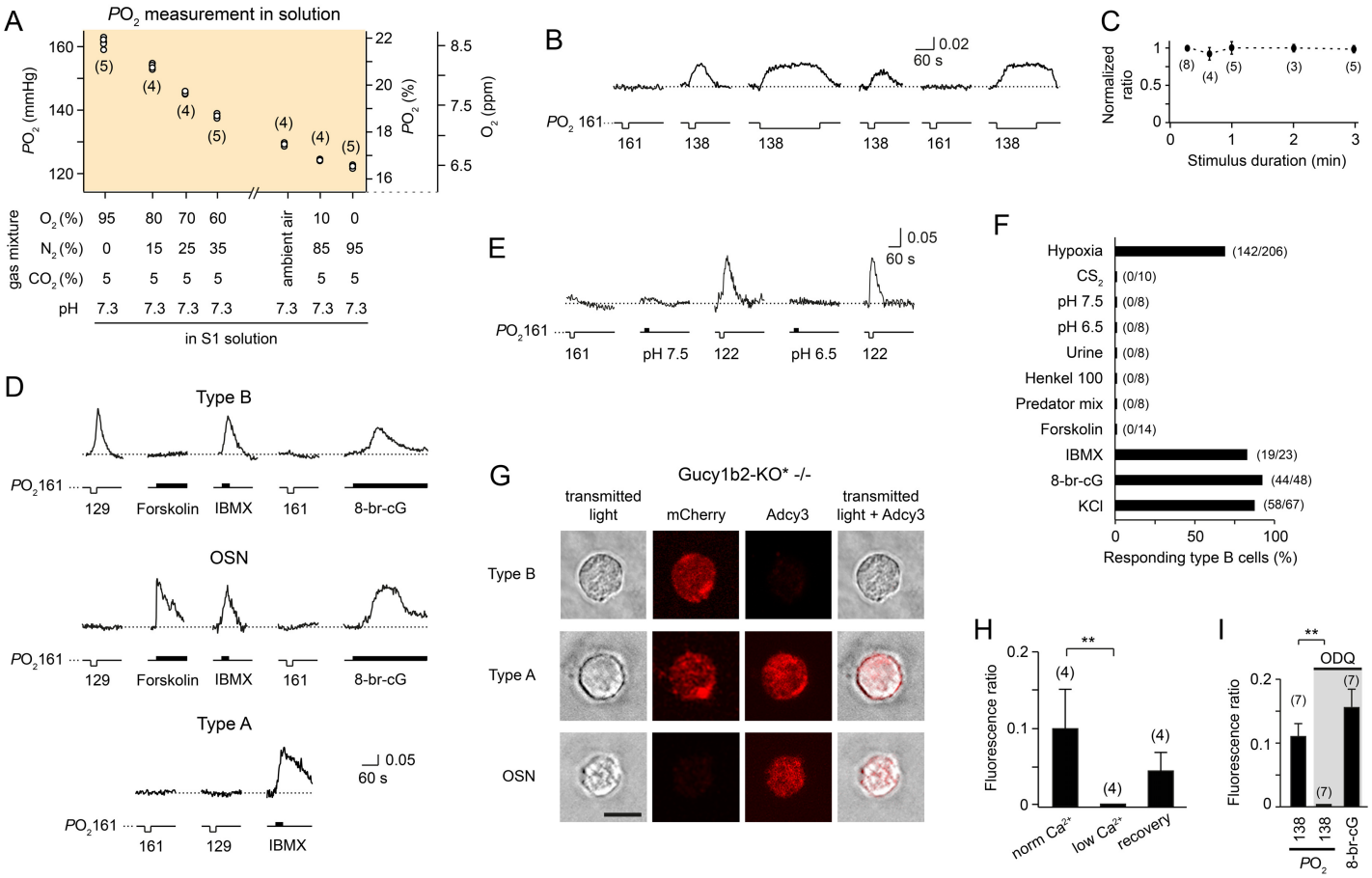
A
PO2 measurement in solution
PO2 (mmHg)
PO2 (%)
O2 (ppm)
gas mixture
O2 (%)
N2 (%)
CO2 (%)
pH
ambient air
in S1 solution
B
0.02
60 s
PO2 161
C
Normalized ratio
Stimulus duration (min)
D
Type B
OSN
Type A
Forskolin
IBMX
8-br-cG
E
0.05
60 s
pH 7.5
pH 6.5
F
Hypoxia
CS2
pH 7.5
pH 6.5
Urine
Henkel 100
Predator mix
Forskolin
IBMX
8-br-cG
KCl
Responding type B cells (%)
G
Gucy1b2-KO* -/-
transmitted light
mCherry
Adcy3
transmitted light + Adcy3
H
Fluorescence ratio
norm Ca2+
low Ca2+
recovery
I
ODQ
PO2
8-br-cG

Figure S1

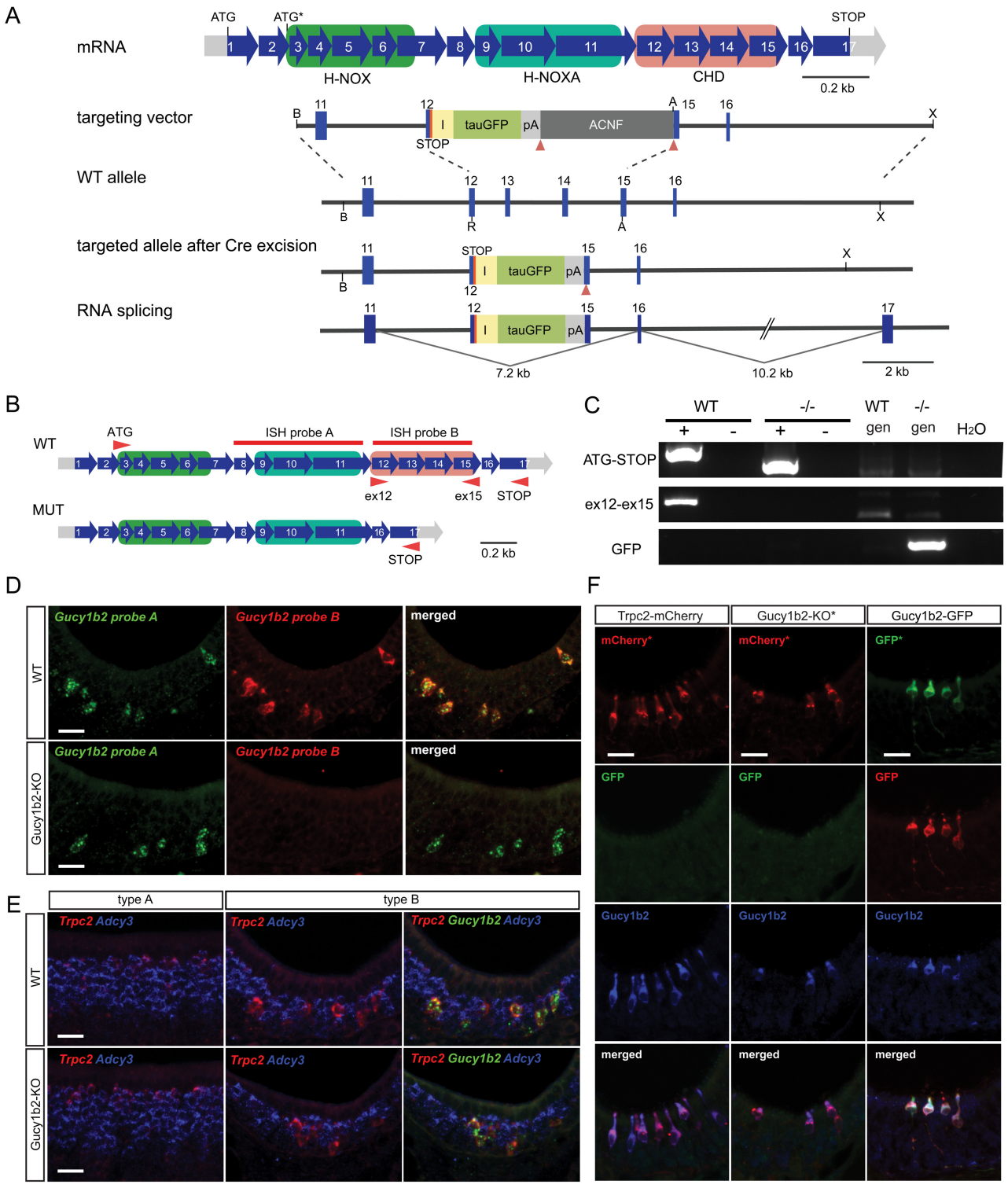
A
mRNA
ATG
ATG*
STOP
H-NOX
H-NOXA
CHD
0.2 kb
targeting vector
tauGFP
pA
ACNF
STOP
WT allele
targeted allele after Cre excision
RNA splicing
7.2 kb
10.2 kb
2 kb
B
WT
MUT
ATG
ISH probe A
ISH probe B
ex12
ex15
STOP
0.2 kb
C
WT
-/-
gen
H2O
ATG-STOP
ex12-ex15
GFP
D
Gucy1b2 probe A
Gucy1b2 probe B
merged
Gucy1b2-KO
E
type A
type B
Trpc2 Adcy3
Trpc2 Gucy1b2 Adcy3
F
Trpc2-mCherry
Gucy1b2-KO*
Gucy1b2-GFP
mCherry*
GFP*
GFP
Gucy1b2
merged

Figure S2

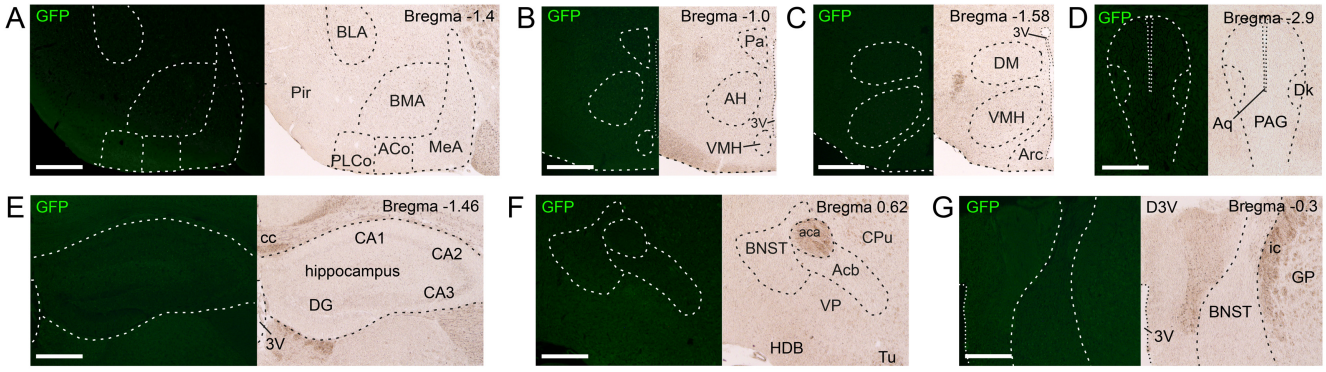
A
GFP
Bregma -1.4
BLA
Pir
BMA
PLCo
ACo
MeA
B
GFP
Bregma -1.0
Pa
AH
3V
VMH
C
GFP
Bregma -1.58
3V
DM
VMH
Arc
D
GFP
Bregma -2.9
Dk
Aq
PAG
E
GFP
Bregma -1.46
cc
CA1
CA2
hippocampus
CA3
DG
3V
F
GFP
Bregma 0.62
aca
CPu
BNST
Acb
VP
HDB
Tu
G
GFP
D3V
Bregma -0.3
ic
GP
BNST
3V

Figure S3

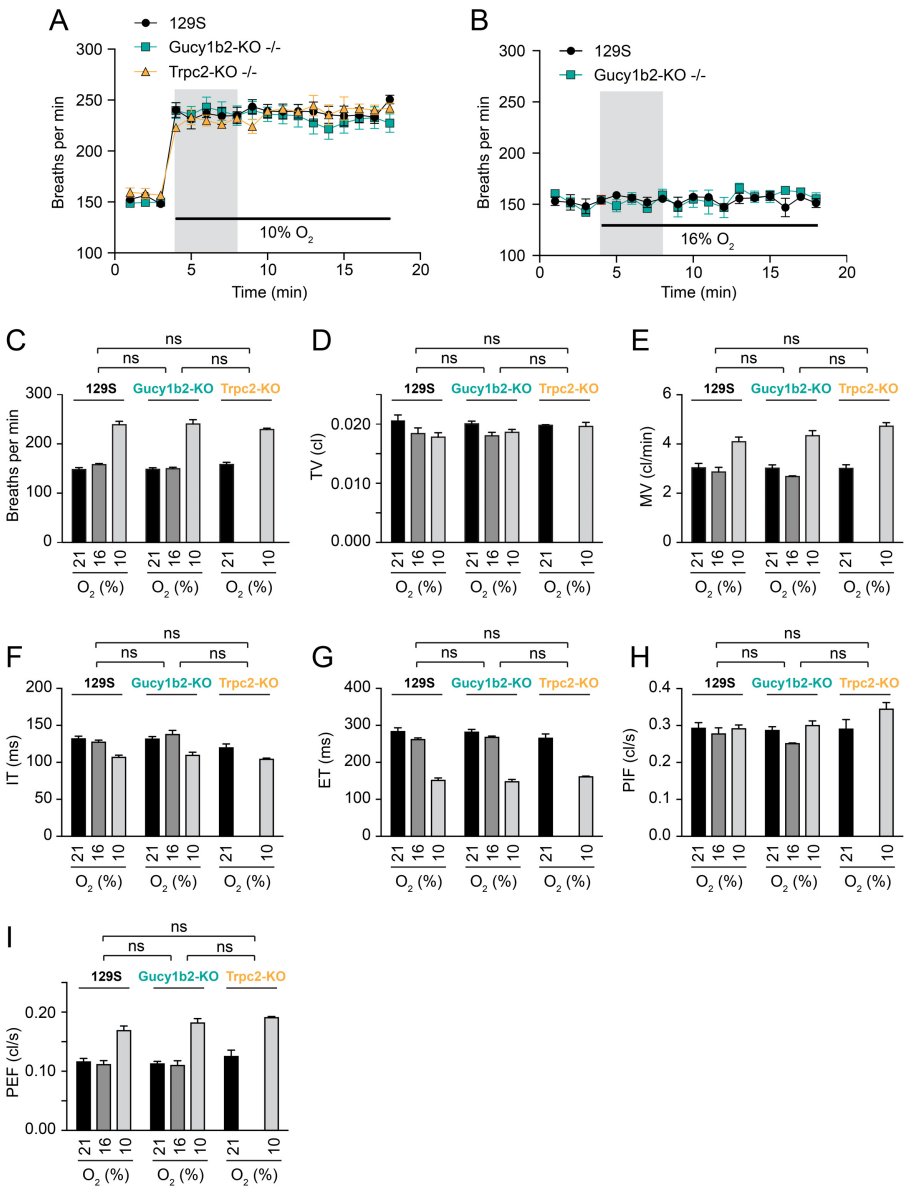
A
129S
Gucy1b2-KO -/-
Trpc2-KO -/-
Breaths per min
Time (min)
10% O2
B
129S
Gucy1b2-KO -/-
Breaths per min
Time (min)
16% O2
C
Breaths per min
D
TV (cl)
E
MV (cl/min)
F
IT (ms)
G
ET (ms)
H
PIF (cl/s)
I
PEF (cl/s)
ns
129S
Gucy1b2-KO
Trpc2-KO
O2 (%)

Figure S4

Figure S1, related to Figure 1.

Properties and Selectivity of Type B Cell Ca^{2+} Responses.

(A) Plot of the oxygen levels measured in extracellular solutions. Various gas mixtures as indicated were bubbled until saturation into S1 solution, keeping the CO_2 concentration and pH constant. Ambient air refers to a solution that was equilibrated in ambient air for at least 2 h at room temperature. Values were measured in ppm or % and converted into PO_2 (mmHg). Dissolved oxygen values were corrected for salinity of the solution. The number of independent measurements obtained on different days is indicated.

(B) Recording example indicating repeatability and effect of stimulus duration on Ca^{2+} responses to low oxygen. Responses were time-locked and there was no evidence for adaptation-like desensitization even after minute-long stimulation.

(C) Peak amplitude of Ca^{2+} responses to low oxygen was independent within the indicated range of stimulus durations. The number of independent recordings is indicated in the graph.

(D) Comparison of response properties of type B cells, canonical OSNs, and type A cells to various stimuli. Type B cells (n = 206) failed to respond to forskolin (50 µM), consistent with their lack of Adcy3 expression. Canonical OSNs (n = 85), which express Adcy3, responded to forskolin but not to low oxygen. Type A cells (n = 10) failed to respond to low oxygen, but responded to IBMX.

(E) Solutions with altered H^+ concentration (pH 7.5 or 6.5) failed to induce a Ca^{2+} response in type B cells.

(F) Summary plot indicating the discrimination capabilities of type B cells and demonstrating that these neurons do not respond to carbon disulfide (CS_2, 13 μM); diluted mouse urine (1:100); a mixture of 100 odorants (Henkel 100, diluted 1:100); and a mixture of several predator odors (see Materials and Methods for details). Results are based on recordings from 42 Gucy1b2-GFP -/- mice. The number of responding versus total cells tested is indicated above each bar.

(G) Examples of posthoc immunostaining of cells from Gucy1b2-KO* -/- mice enabling discrimination among type B cells (mCherry+, Adcy3-), type A cells (mCherry+, Adcy3+), and canonical OSNs (mCherry-, Adcy3+). Scale bar, 10 μm.

(H) Effect of external Ca^{2+} removal on low oxygen responses (122 mm Hg) analyzed in type B cells of Gucy1b2-GFP -/- mice (ANOVA: $F(2, 11) = 10.131$, $p < 0.005$; LSD: ** $p < 0.001$). Partial recovery was evident after restoring external Ca^{2+} concentrations to normal values (LSD: $p = 0.067$). The number of independent recordings is indicated above each bar.

(I) Group data showing type B cell Ca^{2+} responses from Gucy1b2-GFP -/- mice. Treatment with ODQ (10 μM) eliminates the response to low oxygen (138 mmHg) but not to 8-br-cGMP (500 μM).

Results are presented as mean ± SEM.

Figure S2, related to Figure 2.

The Gene-targeted Gucy1b2-D-IRES-tauGFP Mouse Strain.

(A) Targeting scheme of the Gucy1b2-D-IRES-tauGFP mutation. The *Gucy1b2* gene is located on chromosome 14, and consists of 17 coding exons. Functional domains of soluble guanylate cyclases are heme domains H-NOX and H-NOXA, and the cyclase homology domain CHD. The ATG* in the genomic DNA and in the mRNA depicts an alternative *ATG* site in the *Gucy1b2* transcripts identified in RNA extracted from whole olfactory mucosa. A deletion of the catalytic domain CHD of the *Gucy1b2* gene was generated by gene targeting in ES cells. The STOP codon *TGA* was inserted after the *EcoRI* site in exon 12. A segment of 4.3 kb of DNA comprising exon 12 to exon 15, encoding the cyclase homology domain of the Gucy1b2 enzyme, was replaced with an *IRES-tauGFP-pA-ACNF* cassette. The *ACNF* cassette was auto-excised during transmission through the male germline, leaving a single *loxP* site (pink triangle) behind in the genome, and resulting in the Gucy1b2-KO mutation. The exon-intron structure of the major transcript of *Gucy1b2* isolated from whole olfactory mucosa of homozygous Gucy1b2-KO -/- mice (MUT) was analyzed by 3'RACE with primers on exon 11 of *Gucy1b2*. Blue boxes represent exons. A segment of 7.2 kb after exon 11 including the entire *IRES-tauGFP-pA* cassette is spliced out, such that exon 11 is joined to exon 16 in the major transcript of *Gucy1b2* from Gucy1b2-KO mice. As a result, cells that express this mutant allele do not express GFP.

(B) Schematic diagram of the mRNA structure of *Gucy1b2* from wild-type (WT) and mutant (MUT) alleles. The positions of primers used for RT-PCR and riboprobes for ISH are indicated with red arrows and red bars respectively. ISH probe A detects exon 8 to exon 11, a common

region of the WT and MUT transcripts. ISH probe B detects exon 12 to exon 15, a segment that is deleted in MUT transcripts.

(C) RT-PCR analysis of the whole olfactory mucosa of wild-type (WT) and homozygous Gucy1b2-KO -/- mice at 7 weeks with three sets of primers (ATG to STOP, exon 12 to exon 15, and GFP). With the ATG-STOP primer set, a 1.6 kb PCR product was amplified from -/- cDNA compared to the 2.2 kb PCR product from WT. No PCR product was detected from -/- cDNA with the set of primers for exon 12 and exon 15. There is no *GFP* amplifiable from -/- cDNA due to splicing of the whole IRES-tauGFP-pA cassette in *Gucy1b2* transcripts. + , RT+; -, RT-; WT gen, genomic DNA of WT tail; -/- gen, genomic DNA of -/- tail.

(D) In situ hybridization for *Gucy1b2* on coronal sections of the MOE of a wild-type 129S6/SvEvTac mouse and a Gucy1b2-KO -/- mouse (backcrossed 11 times to 129S6/SvEvTac) at 3 weeks. Scale bar, 20 μm.

(E) In situ hybridization for *Trpc2* on coronal sections of the MOE of a wild-type 129S6/SvEvTac mouse and a Gucy1b2-KO -/- mouse (backcrossed 11 times to 129S6/SvEvTac) at 3 weeks. Type A cells express, in addition to *Trpc2*, also *Adcy3* but not *Gucy1b2*. Conversely type B cells express, in addition to *Trpc2*, also *Gucy1b2* but not *Adcy3*. Scale bar, 20 μm.

(F) Immunohistochemistry for GFP and Gucy1b2 of a coronal section of the MOE of a Trpc2-IRES-taumCherry -/- mouse at 10 weeks; a mouse that is Gucy1b2-KO -/- and Trpc2-IRES-taumCherry -/- (Gucy1b2-KO*) at 10 weeks; and a Gucy1b2-GFP -/- mouse at 8 weeks. Type B

cells are Gucy1b2 immunoreactive but immunonegative for GFP due to splicing of the mutant transcripts. Truncated Gucy1b2 protein is expressed in type B cells. The antigen region of the Gucy1b2 antibody (654-675 in the Gucy1b2 sequence) is partially intact in the truncated Gucy1b2 protein in the mutant mouse: it contains 13 amino acids of the 22 amino acids that constitute the antigen region. The Gucy1b2 antibody gives a weaker signal in Gucy1b2-KO -/- mice. The GFP antibody gives a signal (red) in the Gucy1b2-GFP -/- mouse. GFP* and mCherry* show the intrinsic fluorescence of GFP and mCherry. Scale bar, 20 μm.

Figure S3, related to Figure 4.

Absence of GFP Expression in Selected Brain Regions of Gucy1b2-GFP -/- Mice.

Visualization of intrinsic GFP fluorescence (green) in coronal brain sections from Gucy1b2-GFP -/- mice failed to identify labeled cells in amygdala and piriform (Pir) cortex (A), hypothalamus (B, C), periaqueductal grey (PAG; D), hippocampus (E), nucleus accumbens (Acb; F), and bed nucleus of the stria terminalis (BNST; F, G). Transmitted light images (right panels) aid in identifying the various regions as indicated. 3V, third ventricle; ACo, anterior cortical amygdaloid nucleus; AH, anterior hypothalamic area; Aq, aqueduct; BLA, basolateral amygdaloid nucleus; BMA, basomedial amygdaloid nucleus; CA1-3, hippocampus field CA1-3, respectively; cc, corpus callosum; CPu, caudate putamen; D3V, dorsal third ventricle; DG, dentate gyrus; Dk, nucleus of Darkschewitsch; DM, dorsomedial hypothalamic nucleus; fr, fasciculus retroflexus; GP, globus pallidus; HDB, nucleus of the horizontal limb of the diagonal band; ic, internal capsule; MeA, medial amygdaloid nucleus; Pa, paraventricular hypothalamic nucleus; PLCo, posterolateral cortical amygdaloid nucleus; Tu, olfactory tubercle; VMH, ventromedial hypothalamus; VP, ventral pallidum. Scale bar, 400 μm. Distance to bregma zero coordinate is indicated in mm.

Figure S4, related to Figure 4.

Whole-body Plethysmography Reveals Normal Ventilatory Responses to Hypoxia in Gucy1b2-KO -/- Mice and in Trpc2-KO -/- Mice.

(A) Hypoxic ventilatory response of wild-type 129S (129S6/SvEvTac), Gucy1b2-KO -/- (129S6/SvEvTac background) and Trpc2 KO -/- mice (129S6/SvEvTac background) exposed to 10% O_2 for 15 min; n = 9 (129S), n = 10 (Gucy1b2-KO -/-), n = 3 (Trpc2-KO -/-).

(B) Time course illustrating the absence of hyperventilatory response in 129S and Gucy1b2-KO -/- mice exposed to 16% O_2 for 15 min; n = 4 (129S), n = 4 (Gucy1b2-KO -/-).

(C-I) Average respiratory parameters recorded during the first 5 min at 10% O_2 (grey box in (A)) or 16% O_2 (grey box in (B)). There were no significant differences in ventilatory responses to hypoxia between the three genotypes in any of the measured parameters (ANOVA: $F(3,43)$ = 0.713 - 2.208, p = 0.12 - 0.55; ns = non-significant). Tidal volume (TV), minute volume (MV), inspiration time (IT), expiration time (ET), peak inspiratory flow (PIF), peak expiratory flow (PEF); n = 9 (129S), n = 10 (Gucy1b2-KO -/-), n = 3 (Trpc2-KO -/-) for 10% O_2 and n = 4 (129S), n = 4 (Gucy1b2-KO -/-) for 16% O_2 exposures.

Results are presented as mean ± SEM.

SUPPLEMENTAL EXPERIMENTAL PROCEDURES

Mice

Adult (6-23 weeks old) mice (either sex) were kept under standard light/dark cycle (12:12; lights on 0600; lights off 1800) or reverse light/dark cycle (behavioral experiments; 12:12; lights off 0700; lights on 1900) with food and water *ad libitum*. The following strains were used: B6;129P2-*Gucy1b2<tm3Mom>*/MomJ (Stock# 021063; Gucy1b2-IRES-tauGFP, referred to as Gucy1b2-GFP; RRID:IMSR_JAX:021063) (Omura and Mombaerts, 2015); B6;129P2-*Trpc2<tm2Mom>*/MomJ (Stock# 006733; Trpc2-IRES-taumCherry; RRID:IMSR_JAX:006733) (Omura and Mombaerts, 2014); 129S6.129P2-*Trpc2<tm1Mom>*/MomJ (Stock# 007890; Trpc2-KO; RRID:IMSR_JAX:007890) (Omura and Mombaerts, 2014); B6;129P2-*Cnga2<tm1Mom>*/MomJ (Stock# 006644; Cnga2-KO; RRID:IMSR_JAX:006644) (Zheng et al., 2000); B6;129P2-*Gucy1b2<tm2Mom>*/MomJ (Stock# 017517; Gucy1b2-D-IRES-tauGFP, referred to as Gucy1b2-KO; RRID:IMSR_JAX:017517); and 129S6.129P2(B6)-*Gucy1b2<tm2Mom>*/MomJ (Stock# 021844; Gucy1b2-KO backcrossed 10 times to 129S6/SvEvTac; RRID:IMSR_JAX:021844). These strains are publicly available from The Jackson Laboratory. Crossing mice with individual gene-targeted mutations yielded mice that are heterozygous or homozygous for Gucy1b2-KO and homozygous for Trpc2-IRES-taumCherry (referred to as Gucy1b2-KO* +/- or -/-); homozygous for Trpc2 and homozygous for Gucy1b2-GFP (Trpc2-KO* -/-); and hemizygous or homozygous for Cnga2-KO and homozygous for Trpc2-IRES-taumCherry (Cnga2-KO* MUT). Mice carrying the Trpc2-KO mutation and used for whole-body plethysmography were backcrossed 8 times to 129S6/SvEvTac. Mice carrying

only the Gucy1b2-KO mutation were backcrossed 11 times to 129S6/SvEvTac. Mice carrying the Gucy1b2-IRES-tauGFP mutation and all crosses were in a mixed 129 x C57BL/6 background.

Animal care and experimental procedures were performed in accordance with the guidelines established by the German Animal Welfare Act, European Communities Council Directive 2010/63/EU, the institutional ethical and animal welfare guidelines of the Max Planck Institute of Biophysics and the Max Planck Research Unit for Neurogenetics (approval came from the Veterinäramt of the City of Frankfurt), the Saarland University (approval number of the Institutional Animal Care and Use Committee: H-2.2.4.1.1), and the UK Home Office and University of Cambridge. The number of animals used is a minimum necessary to provide adequate data to test the hypotheses of this project. We have minimized the number of animals required by the animal welfare committees wherever possible.

En face imaging of GFP+ neurons in the MOE

Gucy1b2-GFP -/- mice (6 weeks to 14 months old) were used. Mice were anesthetized by injection of ketamine HCl and xylazine (210 mg/kg and 10 mg/kg body weight) and decapitated. The MOE was peeled off from the lateral turbinate, and transferred into Ringer's solution (140 mM NaCl, 5 mM KCl, 1 mM $CaCl_2$, 1 mM $MgCl_2$, 10 mM Hepes, 10 mM glucose, 1 mM Na pyruvate, pH 7.4). The MOE sample was flattened by trimming, transferred to a tissue slice chamber (Warner instruments) with the cilia layer facing up, and fixed with a stainless steel slide anchor. En face view images of the GFP+ neurons were collected with a Zeiss LSM710 confocal

microscope (Axio Imager Z1) equipped with an Achroplan 100x/1.00 water-immersion objective (Zeiss).

Calcium imaging

For Ca^{2+} imaging experiments, mice (6-23 weeks old) were decapitated following anaesthesia. Cells were freshly dissociated from the MOE without the use of enzymes during the dissociation procedure. The turbinates were dissected carefully out of the nasal cavity and minced in low Ca^{2+}-solution containing (in mM): 120 NaCl, 25 $NaHCO_3$, 5 KCl, 4.25 $CaCl_2$, 5 EGTA, 1 $MgCl_2$, 5 BES, pH = 7.3, 300 mOsm. Minced tissue was incubated in this solution for an additional 15 min (37°C) and then gently passaged using a fire-polished Pasteur pipette and oxygenated solution S1 (95% O_2/ 5% CO_2; RT = 21°C) consisting of (in mM): 120 NaCl, 25 $NaHCO_3$, 5 KCI, 1 $MgSO_4$, 1 $CaCl_2$, 10 Glucose, 5 BES, pH 7.3, 300 mOsm. Dissociated cells were placed on coverslips previously coated with poly-L-lysine (0.01%) and laminin (0.1%) and incubated in oxygenated S1 solution containing the ratiometric Ca^{2+}-indicator fura-2/AM (6 µM, Invitrogen), 0.01% Pluronic-F127 (Invitrogen) and 0.67% DMSO for 30 min at RT. Coverslips containing fura-2 loaded cells were placed in a laminar flow recording chamber (RC-27, Warner Instruments) and continuously perfused with oxygenated S1 solution at a rate of ~ 10 µl/s (RT). Ca^{2+} imaging was performed using an upright microscope (Olympus BX-51WI) equipped with a 20x/1.00 water immersion objective (XLUMPlanFL N) and a CCD camera (ORCA-R2, Hamamatsu Photonics). Fura-2 ratios were determined at 340 and 380 nm. Image pairs were acquired at 0.5 Hz and analyzed using ImageJ (NIH) and Igor Pro software (Wavemetrics) as described (Pérez-Gómez et al., 2015; Schmid et al., 2010). Chemostimuli were prepared freshly

each day and diluted in oxygenated solution S1 giving the following final concentrations: Henkel 100 containing a mixture of 100 volatile odorants (1:100; Henkel) from several classes and groups such as aromatics, aliphatics, alcohols, aldehydes, esters, ethers, ketones, amines, alkanes, heterocyclics and others (Wetzel et al., 1999); urine from C57BL/6 male mice, 1:100; predator odor mix (2-PT, 2-propylthietane; TMT, 2,5-dihydro-2,4,5-trimethylthiazole; PEA, ß-phenylethylamine; 2,6-DMP, 2,6-dimethylpyrazine; each at 100 µM) (Pérez-Gómez et al., 2015); CS_2, 13 µM; forskolin, 50 µM; IBMX (3-isobutyl-1-methylxanthine), 100 mM; 8-br-cGMP (8-bromoguanosine 3',5'-cyclic monophosphate), 500 µM; and KCl, 30 mM. Stimuli were bath-applied in random order. If not otherwise stated, stimulus duration was 20 s. For IBMX and KCl, we used 30-s stimuli; forskolin and 8-br-cGMP were applied for 2 min or sometimes longer. KT5823 (10 µM; CAS# 126643-37-6) and ODQ (1H-[1,2,4]oxadiazolo[4,3-a]quinoxalin-1-one; 10 µM; CAS# 41443-28-1) were obtained from Tocris. L-NAME (N_ω-nitro-L-arginine methyl ester hydrochloride) was obtained from Sigma. Cells were treated with these compounds for 10-15 min. ODQ (1H-[1,2,4]oxadiazolo[4,3-a]quinoxalin-1-one; CAS# 41443-28-1) was obtained from Tocris. Experiments with reduced external Ca^{2+} concentrations used oxygenated S1 solution buffered with 1 mM EGTA (ethylene glycol-bis(2-aminoethylether)-N,N,N′,N′-tetraacetic acid) and no added Ca^{2+}. Unless otherwise stated chemicals were purchased from Sigma.

Oxygen measurements and calibration

Oxygen levels were adjusted by bubbling S1 solution with gas mixtures until reaching saturation or by delivering a steady stream of gas mixtures to the behavioral chambers until reaching

equilibrium. Dissolved oxygen was measured with an oxygen electrode calibrated for temperature of the solution and atmospheric pressure (GMH3630, Greisinger electronic GmbH, Germany). Values were corrected for the salinity of the solutions (Rounds et al., 2013). S1 solution oxygenated with 95% O_2, 0% N_2, 5% CO_2 resulted in an average PO_2 of 161 mmHg. For the in vivo experiments, we used a dedicated gas detector (X-am 5000, Dräger, Germany) to measure actual O_2 and CO_2 levels in the environmental air of our behavioral chambers. Electrodes were calibrated before each measurement according to the manufacturer's instructions. PO_2 values in the figures refer to the mean value determined from independent measurements obtained on different days before an experiment.

Posthoc immunostaining of cells from Gucy1b2-KO* and Cnga2-KO* mice

To discriminate type B cells from type A cells in Gucy1b2-KO* and Cnga2-KO* mice, posthoc immunostaining was performed following Ca^{2+} imaging directly in the recording chamber (Chamero et al., 2011), in order to distinguish Trpc2+ Adcy3- (type B) cells versus Trpc2+ Adcy3+ (type A) cells. Dissociated cells were fixed using phosphate-buffered saline (PBS) containing 4% paraformaldehyde (PFA) for 10 min at RT, permeabilized and incubated for 10 min in blocking solution [4% horse serum, 1% bovine serum albumin fraction V (Roth), 0.3% Triton X-100 in PBS], incubated with rabbit anti-Adcy3 (1:1000, 1 h, room temperature, SC-588, Santa Cruz, RRID:AB_630839), and washed in blocking solution (5 min) followed by an incubation with secondary antibody (1:800, 30 min, room temperature, Alexa Fluor 633 goat anti-rabbit, Thermo Fisher Scientific, RRID:AB_2535731).

Generation of the Gucy1b2-D-IRES-tauGFP (Gucy1b2-KO) strain

To generate the targeting vector for the Gucy1b2-KO mutation, a 4.2 kb *BamHI-EcoRI* fragment containing exon 11 and part of exon 12 (left homology arm) and a 7.2 kb *AccIII–XhoI* fragment containing part of exon 15 to the intron between exon 16 and exon 17 (right homology arm) were isolated from bacterial artificial chromosome clone bMQ-312D1 (Source Bioscience). A *STOP-PacI-IRES-tauGFP-pA-ACNF-PacI* cassette was inserted between the arms. This design results in a deletion of a 4.3 kb segment of genomic DNA containing part of exon 12 to part of exon 15 and encoding the entire cyclase homology domain (CHD) of *Gucy1b2*. Embryonic stem cells from parental line E14 were electroporated with the linearized targeting vector. G418-resistant clones were screened by Southern blotting using a 5' external probe (nucleotides 62413377-62413847 from NC_000080.6, *AseI* digestion of genomic DNA) and a 3' external probe (nucleotides 62396184-62396756 from NC_000080.6, *DraI* digestion). Targeted ES clones were injected into C57BL/6J blastocysts, chimeras were bred with C57BL/6J mice, and a strain established from targeted ES cell clone 4-187 initially in a mixed 129 x C57BL/6 background. An inbred strain called Gucy1b2-D-IRES-tauGFP (129S6/SvEvTac-N11) was then generated by eleven backcrosses to 129S6/SvEvTac. Mice were maintained in specified pathogen-free conditions in individually ventilated cages of the Tecniplast green line.

RT-PCR

Total RNA was extracted from the lateral part of the whole olfactory mucosa of two Gucy1b2-KO -/- mice and two +/+ littermates in a mixed 129 x C57BL/6 background at 7 weeks with

TRIzol reagent (Thermo Fisher Scientific). DNaseI-treated total RNA was purified with RNAeasy columns (Qiagen) followed by clean up protocol. Purified total RNA was reverse-transcribed using Superscript III (Thermo Fisher Scientific) with oligo dT $_{(20)}$ primer (Thermo Fisher Scientific). For amplification of the *Gucy1b2* gene, two set of primers were used, ATG-STOP (ATG; *ATGTACGGATTTATCAACACCT*, STOP; *TCACAACACAGCACAGAAGGCA*) and ex12-ex15 (exon 12; *GAGAATTCGAGACGTGTACC*, exon 15; *CCTTCCCATCAGCGAGAGCTG*). To check GFP expression, PCR was performed with GFP-for; *GCATCAAGGTGAACTTCAAGATCCG* and GFP-rev; *AGCTCGTCCATGCCGAGAGTGATC*.

3'-Rapid amplification of cDNA end (3'-RACE) analysis

To investigate the transcript structure of *Gucy1b2* in the whole olfactory mucosa, 3'-RACE was performed using the SMARTer RACE cDNA amplification kit (Clonetech Laboratories) according to manufacturer's protocol. Briefly, total RNA was extracted from lateral whole olfactory mucosa of Gucy1b2-KO -/- and +/+ littermates in a mixed 129 x C57BL/6 background at 7 weeks, and was used as template for first strand cDNA synthesis. The 3'-RACE reactions were performed in two steps. First amplification was performed with RACE-ex10-11; *GCCAGCCGACACTCAAACTCCGGGGTC* and Universal Primer A Mix (Clontech Laboratories), then a nested reaction was performed with Nested Universal Primer A (Clontech Laboratories), and RACE-ex11-1; *CATCGCTCCCCACGACACGACCAGGG* or RACE-ex11-2; *CATGTGGCCAACCAGCTCAAGGAGGG*. Amplified PCR products were cloned into pGEM-T-easy vector (Promega) and sequences were analyzed.

In situ hybridization

Three-week old Gucy1b2-KO -/- mice and 129S6/SvEvTac wild-type mice were analyzed. Dissection, sample preparation, and ISH were performed as described (Ishii et al., 2004). ISH probe A was prepared from exon 8 to exon 11 of *Gucy1b2* (nucleotides 965-1673 from NM_172810.3), and ISH probe B was prepared from exon 12 to exon 15 (nucleotides 1719-2321 from NM_172810.3). The *Trpc2* and *Adcy3* riboprobes have been described (Omura and Mombaerts, 2014). Images were collected with a Zeiss LSM 710 confocal microscope.

Immunohistochemistry of the MOE

Immunohistochemistry was performed as described (Omura and Mombaerts, 2015). Mice were Trpc2-IRES-taumCherry -/- at 10 weeks; Trpc2-IRES-taumCherry -/- and Gucy1b2-KO -/- at 10 weeks; and Gucy1b2-GFP -/- at 8 weeks. The following primary antibodies were applied: rabbit anti-Gucy1b2 (1:500) (Omura and Mombaerts, 2015), and chicken anti-GFP (1:1000, GFP-1020, Aves Labs, RRID:AB_10000240). After one overnight incubation with primary antibodies at 4°C, sections were incubated at 1.5 h at room temperature with secondary antibodies: donkey anti-rabbit IgG-Alexa647 (1:500, 711-606-152, Jackson ImmunoResearch Laboratories, RRID:AB_2340625) for rabbit anti-Gucy1b2, donkey anti-chicken IgY-Alexa488 (1:2000, 703-545-155, Jackson ImmunoResearch Laboratories, RRID:AB_2340375) for chicken anti-GFP on the sections of Trpc2-IRES-taumCherry and donkey anti-chicken IgY-Rhodamine Red X (1:1000, 703-295-155, Jackson ImmunoResearch Laboratories, RRID:AB_2340371) for chicken

anti-GFP on the sections of Gucy1b2-GFP -/- mice. Sections were analyzed with a Zeiss LSM 710 confocal microscope.

Analysis of GFP expression in brain sections of Gucy1b2-GFP -/- mice

Gucy1b2-GFP -/- mice at 8 weeks (n = 3) were transcardially perfused with 4% PFA in PBS. Tissue was dissected, post-fixed for 2 h and equilibrated overnight in PBS containing 30% sucrose at 4°C. Brains were snap-frozen in a dry ice/2-methylbutane bath. Coronal sections (18 µm) were collected on a cryostat (Microm HM525) and mounted onto SuperFrost Plus glass slides. GFP fluorescence was visualized using both intrinsic GFP fluorescence and anti-GFP immunostaining. Both methods gave the same results. Immunohistochemical procedures were conducted at room temperature, with the exception of primary antibody incubations (4°C). The following primary and secondary antibodies were used: chicken anti-GFP (1:1000, ab13970, Abcam, RRID:AB_300798) and goat anti-chicken IgG-Alexa Fluor-555 (1:1000, A-21437, Life Tech, RRID:AB_2535858). All sections were counterstained with Hoechst 33342 (1:10000) and mounted with DAKO fluorescent mounting medium. Fluorescence images were acquired on an Olympus IX71 microscope. Anatomical limits of selected brain regions were outlined in all sections by superimposing nuclear counterstains onto transmitted light images and using a mouse brain atlas (Paxinos and Franklin, 2001). As key landmarks we used selected brain structures including hippocampus, optic tract, fornix, third ventricle, internal and external capsule, lateral ventricle, anterior and posterior commissure, olfactory tubercle, lateral olfactory tract, nucleus of Darkschewitsch, and piriform cortex.

Imaging c-Fos immunoreactivity in olfactory bulb neurons

Singly-housed mice kept in reverse light/dark cycle for at least one week were habituated to a behavioral chamber (26×17×21 cm Makrolon polycarbonate box with lid) for 3 days (30 min each day). The chamber contained an entry port for gas mixture delivery (standard control gas mixture: 20% O_2, 80% N_2; flow rate: 3 l/min) and an exhaust port. On day 4, mice were exposed first to a gas mixture containing 20% O_2 for 30 min and subsequently to either a low oxygen containing gas mixture (16% O_2, 84% N_2) or the 20% O_2 gas mixture for an additional 10 min. All training and testing procedures were monitored using video recording. After oxygen exposure mice were returned to their home cage for 90 min to enable c-Fos accumulation before anesthetizing (195 mg/kg body weight ketamine and 18 mg/kg body weight xylazine) and transcardially perfusing the mice with 4% PFA in PBS. Tissue was dissected, post-fixed for 2 h and equilibrated overnight in PBS containing 30% sucrose at 4°C. Olfactory bulbs were snap-frozen in a dry ice/2-methylbutane bath. Sagittal sections (18 µm) were collected on a cryostat (Microm HM525) and mounted onto SuperFrost Plus glass slides. Immunohistochemical procedures were conducted at room temperature, with the exception of primary antibody incubations (4°C). The following primary and secondary antibodies were used: for Gucy1b2-GFP -/- mice, goat polyclonal anti-c-Fos (1:200, sc-52-G, Santa Cruz Biotechnology, RRID: AB_2629503) and Alexa Fluor-546 donkey anti-goat (1:500, A-11056, Life Tech, RRID:AB_2534103); for Gucy1b2-KO* mice, rabbit anti-RFP (1:500, 600401379, Rockland, RRID:AB_2209751), goat polyclonal anti-c-Fos (1:200, sc-52-G, Santa Cruz Biotechnology, RRID: AB_2629503), Alexa Fluor-555 donkey anti-rabbit (1:500, A-31572, Life Tech, RRID:AB_162543) and Alexa Fluor-488 donkey anti-goat (1:500, A-11055, Life Tech,

RRID:AB_2534102). Sections were incubated with Hoechst 33342 (1:10,000) and mounted with DAKO fluorescent mounting medium. Through the nuclear staining, the boundaries of densely packed cells in the vicinity of a given GFP+ or mCherry+ glomerulus were defined and c-Fos immunoreactive cells within this area were counted (Pérez-Gómez et al., 2015). These cellular counts (mean number of nuclei/mm^3) were evaluated blindly for each mouse.

Conditioned place aversion

Experiments were conducted in a custom-made arena composed of two chambers of equal size (26×17×21 cm each; Makrolon polycarbonate box with lid) with a connecting opening (5 cm wide, 4 cm high). The opening could be closed by a sliding door to limit accessibility to only one chamber. Both chambers contained a port for gas mixture delivery (standard control gas mixture: 20% O_2, 80% N_2; low oxygen gas mixture: 16% O_2, 84% N_2; flow rate: 3l/min) and an exhaust port. A tube was affixed to the gas mixture delivery port outside each chamber. For each chamber, we used a separate, computerized QCAL gas mixing system (GMS_3CH, Oberostendorf, Germany) operated by dedicated software (version 4.3). The arena was surrounded by contextual cues (high-contrast geometric objects located on the walls surrounding the chambers). The conditioned place aversion protocol included preconditioning, conditioning, and testing phases. During preconditioning (performed across 3 days) all mice were allowed to explore the environment (both chambers) for 30 min per day. Following preconditioning, mice underwent conditioning for 3 days with alternating treatment-chamber pairings during the morning and afternoon. During the conditioning phase, mice were placed in the paired chamber without access to the other compartment. Each chamber was dedicated to contain either the gas

mixture (20% O_2, control chamber) or the low oxygen gas mixture (16% O_2, low-oxygen chamber). Half of the mice were placed into the control chamber in the morning, followed by placement in the low-oxygen chamber in the afternoon. The other half of the mice were treated in the reverse order. Morning and afternoon sessions were separated by ≥ 3 h. The position of the low-oxygen chamber was randomized across trials and mice, relative to the visual cues outside the arena. On the test day, mice were placed into the 16%-paired chamber and had access to both chambers (but both now at 20% O_2) for 10 min. Behavior was recorded and automatic tracking was performed by reducing the speed of the digital videos to 1 frame/s. After a thresholding step to 8-bit B/W (binary contrast enhancement), particles were 2D-analyzed using ImageJ (NIH) Mtrack2. A reduction of the time spent in a chamber associated with 20% or 16% O_2 exposure indicated aversion of the condition. Preference index was calculated as the difference between the time a given mouse spent in the low-oxygen chamber (t16) and the time the same mouse spent in the control chamber (t20) as follows: (t16 - t20)/(t16 + t20). For statistical analysis, a one-sample t test against 0.0 was used. Multiple groups were compared using a two-way analysis of variance (ANOVA) with the Fisher's least significant difference (LSD) as a posthoc comparison.

Morris water maze

Mice were 7-16 weeks old. A plastic circular pool (120 cm in diameter) filled with tepid water (23°C ± 1°; depth, 30 cm) was made opaque using non-toxic white paint (VBS Hobby Service GmbH, Germany). Trial starting points were marked outside the pool as north (N), south (S), east (E), and west (W), dividing the maze into four equal quadrants (NE, SE, SW, NW). A

circular transparent platform (diameter, 10 cm) was submerged to ~1 cm below the surface, and was kept in a fixed position. To locate this hidden escape platform, mice had to rely on four distant visual cues placed on each wall of the water maze room. Mice were trained to find the platform for eight trials per day (two non-consecutive blocks of four trials with starting points selected pseudo-randomly) and, once the platform was located, they were allowed to stay on it for 20 s before the next trial started. If a mouse did not find the platform within 60 s, the animal was gently guided to it and a score of 61 s was recorded for that trial. Latencies-to-find-platform were measured in each training session. For testing reference memory, single probe trials were carried out 24 h after the last training session. Mice were released at a random starting positions and were allowed to swim during 60 s in the absence of the platform. All trials were video recorded for later off-line analysis.

Whole-body plethysmography

Respiratory parameters were measured by unrestrained whole-body plethysmography (Data Sciences International) as in Macías et al., 2014. Mice were maintained in a hermetic chamber with controlled normoxic airflow (1.1 l/min 20.5% O_2, 0.5% CO_2, 79% N2) until they were calm. Mice were then exposed to pre-mixed hypoxic air (1.1 l/min) of 16% O2 (and 84% N2) or 10% O_2 (and 90% N2) (BOC Healthcare) for 15 min. Real-time data were recorded and analyzed using Ponemah software (Data Sciences International). Each mouse was monitored throughout the experiment and periods of movements and/or grooming were noted and subsequently removed from the analysis. The transition periods between normoxia and hypoxia (3 min) were also removed from the analysis.

Statistics and data analysis

Statistical analysis was performed using SPSS software. One-way analysis of variance (ANOVA) with Fisher´s least significant difference (LSD) as post hoc comparisons was used to evaluate multiple groups with one independent variable. Multiple groups with two independent variables were compared using two-way ANOVA with LSD as post hoc comparison. Results are presented as means ± SEM.

Supplemental References

Ishii, T., Omura, M., and Mombaerts, P. (2004). Protocols for two- and three-color fluorescent RNA in situ hybridization of the main and accessory olfactory epithelia in mouse. J. Neurocytol. *33*, 657-669.

Paxinos, G., Franklin, K.B. (2001). The Mouse Brain in Stereotaxic Coordinates. Second Edition. Elsevier Academic Press.

Rounds, S.A., Wilde, F.D., and Ritz, G.F. (2013). Dissolved oxygen (ver. 3.0): In National Field Manual for the Collection of Water-Quality Data (U.S. Geological Survey Techniques of Water Resources Investigations), Chapter 6, pp. 1-55.

Schmid, A., Pyrski, M., Biel, M., Leinders-Zufall, T., and Zufall, F. (2010). Grueneberg ganglion neurons are finely tuned cold sensors. J. Neurosci. *30*, 7563-7568.